

## Geochemistry of Sandstones from the Alma and Swaershoek Formations (Waterberg Group) and the Glentig Formation, South Africa: Implications for Tectonic Provenance and Paleoweathering

Melton Makulana, Samson Masango and Christopher Baiyegunhi\*

Department of Geology and Mining, University of Limpopo, Private Bag X1106, Sovenga 0727, Limpopo Province, South Africa

Received January 25, 2023; Accepted June 19, 2023

---

### Abstract

The Wolkberg, Chuniespoort, and Pretoria Groups are currently defined as the Transvaal succession in the eastern Transvaal, southern Africa and are succeeded by the Rooiberg and Waterberg Groups. The Waterberg Group is a clastic sedimentary succession that is present across the northern part of the Kaapvaal Craton and was deposited during the late Palaeoproterozoic. The Glentig Formation, which was laid down in the remnants of the shrinking Transvaal basin, represents the final stage of the Transvaal cycle. The Glentig Formation was previously classified as part of the uppermost Pretoria Group, but it is now considered a proto-Waterberg unit. The Swaershoek and Alma Formations (Waterberg Group) overlie the unconformity-bounded Glentig Formation. These formations developed during the Bushveld igneous complex's volcanic activity (BIC). Previous research only correlated the Glentig Formation with the Swaershoek and Alma Formations. However, neither the source rock characteristics nor the tectonic provenance of these formations have been studied in the past. In order to fill the gaps, the geochemistry of rocks of the above mentioned formations were studied to determine their source rock characteristics, provenance, and tectonic setting. Petrographic analysis indicates that the detrital components of the sandstones are dominated by quartz. Provenance analysis indicates that the sandstones are derived mostly from felsic igneous rocks, with little input from intermediate igneous rocks. The abundance of quartz relative to feldspar and rock fragments in the formations is consistent with a felsic-dominated provenance. Major and trace element geochemical results display a high SiO<sub>2</sub> component in all samples, as well as enrichments in Th and especially Zr. Tectonic setting discrimination diagrams show that the sandstones are from both passive and active continental margin tectonic settings. The chemical index of weathering (CIW), chemical index of alteration (CIA) and plagioclase index of alteration (PIA) and ternary diagram of Al<sub>2</sub>O<sub>3</sub>–(CaO+Na<sub>2</sub>O)–K<sub>2</sub>O (represented as A–CN–K) suggest that the source area of the sandstones was subjected to moderate to intense weathering conditions.

**Keywords:** Geochemistry; Provenance; Tectonic setting; Glentig Formation; Waterberg Group.

---

## 1. Introduction

The Swaershoek and Alma Formations are the Paleoproterozoic Waterberg Group's oldest red-bed formations [1]. The Swaershoek Formation outcrops north of Modimolle town in the Limpopo Province, and it is conformably overlain by the Alma Formation along the Swaersberg Mountains' east-west strike (Figure 1). Conglomerates and sandstones dominate the formations, which are periodically intruded by quartz-feldspar porphyries. The Swaershoek Formation overlies the Glentig Formation in the eastern Swaersberg Mountains. Previous geological investigations in South Africa, particularly in the Waterberg and Rooiberg Groups, have mostly focused on the economically viable lithologies, with less attention paid to other formations such as the Glentig, Swaershoek, and Alma Formations [2-3]. These units are depositional sequences, thus they are referred to as "chronostratigraphic units" [4].

---

The mineralogical composition of clastic sedimentary rocks is controlled by several factors that include source rock composition, chemical and physical weathering, and sedimentation processes (i.e., mechanical sorting decomposition and diagenesis) [5]. The chemistry of siliciclastic sedimentary rocks has been long used for unravelling the source rock compositions, paleoclimatic conditions and tectonic setting. Several researchers [6-10] have studied the composition of siliciclastic sediments and their tectonic setting and provenance all over the world. The geochemistry of siliciclastic sedimentary rocks can display traits about the parent materials. Furthermore, weathering, transportation, and diagenesis are some of the determining factors of the chemical composition of clastic rocks. Emphasis has been put on the comparatively immobile elements such as Cr, Co, Th, Y, Zr, Hf, Nb and Sc [11]. The relatively low mobility of these elements during sedimentary processes allows or supports the discrimination between different tectonic provenances and paleoweathering conditions.

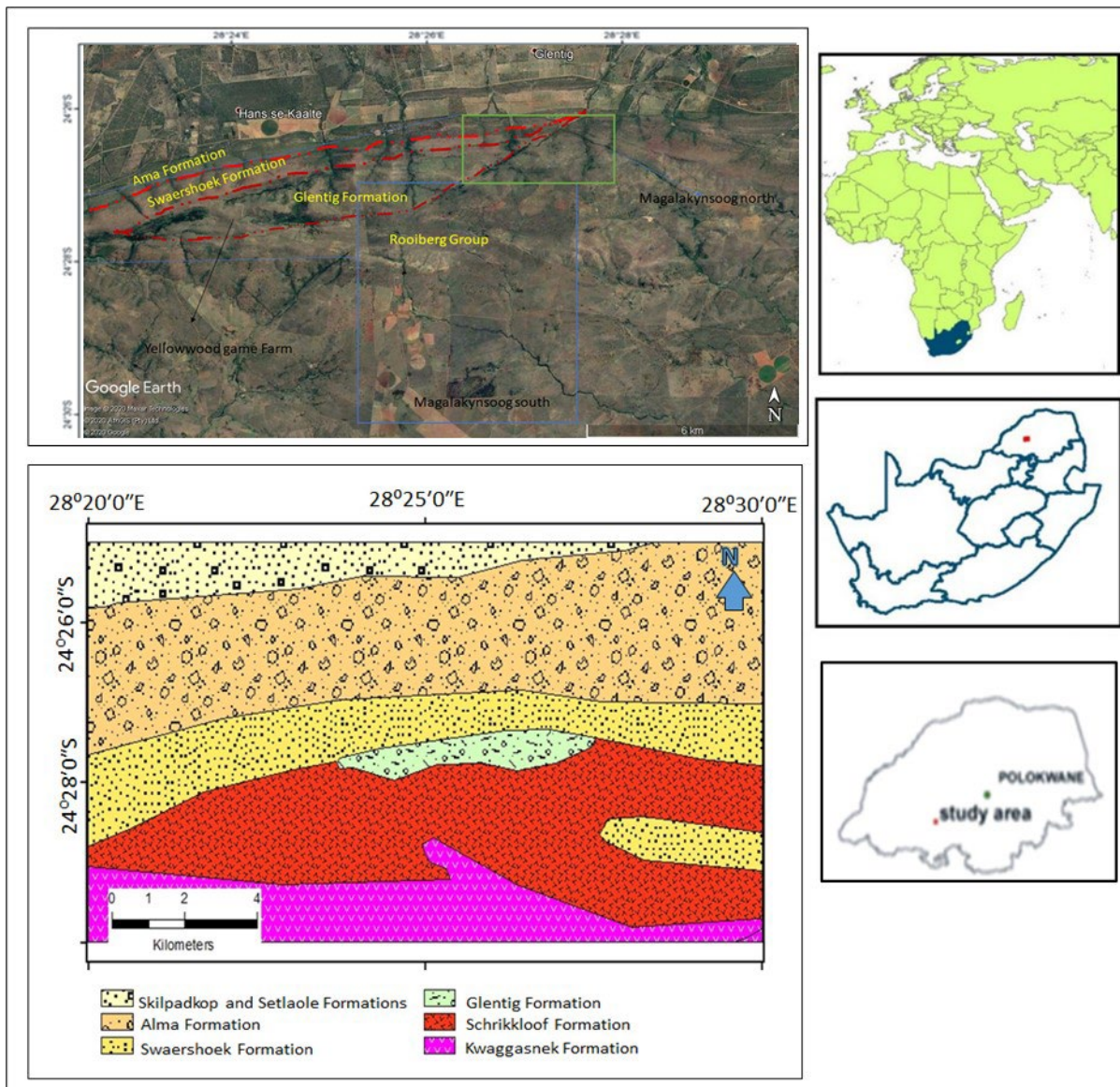


Figure 1. Map showing the study area and relationships of the Glentig Formation and Swaershoek, and Alma Formations (Waterberg Group) north of Modimolle town, Limpopo (after [30]). Note: The blue and green lines in the inserted Google image show the farm boundaries

In recent years, the use of geochemical techniques has advanced the determination of provenance of sediments. Sediments are deposited in three major sites or areas, namely, the

active continental margin, passive continental margin and Island arc [9]. The factors that control the mineralogical composition of clastic sedimentary rocks include (1) the composition of their source rocks, (2) environmental parameters influencing the weathering of source rocks (i.e., atmospheric chemistry, temperature, rainfall and topography), (3) duration of weathering, (4) transportation mechanisms of the clastic material from the source region to depocentre, (5) depositional environment (e.g., marine versus freshwater), and (6) post-depositional processes (i.e., diagenesis, metamorphism) [12]. Several investigations have substantiated the above aspects of the genesis of both ancient and modern siliciclastic sediments [6,8,13-22]. Quite a number of studies have also been focused on the identification of palaeo-tectonic settings of provenances based on the geochemical signatures of siliciclastic rocks [6-8]. Herein, the major and trace element geochemistry of the sandstones were used to determine provenance and tectonic setting of the investigated formations.

The Glentig, Swaershoek, and Alma Formations are among South Africa's least studied geological formations. Previous research on the Alma, Swaershoek, and Glentig Formations focused mostly on the formations' stratigraphy and age [2,4,23-30]. The Alma Formation is deposited in the main Waterberg Basin and it is mainly composed of sandstones and shale with a total thickness of about 300 m thick [28]. The Swaershoek is the basal unit of the Waterberg Group in the Nylstroom Protobasin, and it is mainly made up of sandstones with interbedded conglomerates and breccias [24]. Research works by [27-28] are the only documented studies on the Glentig Formation. The Glentig Formation is a proto-Waterberg / Soutpansberg unit, according to the South African Committee on Stratigraphy [2,4]. The Glentig Formation's tectonic context and depositional environment are not well studied, and its provenance is poorly understood. Despite the fact that considerable research has been done on the Swaershoek and Alma Formations, their provenance, tectonic setting, and source rock characteristics remain poorly documented. Hence, this study used major and trace element composition of the sandstones from the formations described above to provide information on the source rock characteristics, provenance, paleoweathering, and tectonic setting. The findings of this study could be utilized to deduce an interpretation of the basin's sedimentary history and evolution, as well as improve our understanding of the evolution of geological events that occurred in southern Africa during the previous 2 billion years.

## 2. Geological setting

During the Paleoproterozoic (2-0.85 Ga) age, the Waterberg Group was deposited in gradually subsiding intra-cratonic basins in the north of the Kaapvaal Craton [1]. The group was formed primarily by alluvial/braided-fluvial processes in a secondary paleo-desert environment, within fault-bounded, perhaps pull-apart basins [31]. The Waterberg Group is one of the earliest known red-bed occurrences in South Africa, and it is part of the red-bed successions that are common in southern Africa [32]. These red layers, which have an average thickness of around 8.5 km, are sourced from the Transvaal Supergroup and the Bushveld Complex [33]. The Waterberg Group clastic sediments were deposited unconformably over the Blouberg Formation, Transvaal Sequence, Bushveld Complex granite and mafic rocks, and the Archean basement of the Kaapvaal Craton [34]. The ages of the Waterberg Group is constrained within the age limits of 2.06-1.88 Ga [2]. Conversely, [32] reported the age of the Waterberg Group to be  $2054 \pm 4$  Ma. Catuneanu *et al.* [31] indicated that the Waterberg Group was deposited between the time frame of 3.0 to 1.8 Ga, whereas [34] presented the age of the Waterberg Group to be 1800-1900 Ma. The Waterberg Group is preserved within the Main and Middleburg Basin on the Kaapvaal Craton and it was deposited largely by alluvial/braided-fluvial with the secondary paleo-desert environment, within fault-bounded, possibly pull-apart type depositories [31]. The Waterberg Group's "red beds" are preserved in two major structural domains of the Kaapvaal Craton. They are an east-west elongated domain bounded to the north by the Zoetfontein-Melinda faults and to the south by the Thabazimbi-Murchison Lineament (TML) (Figure 2). The Central Bushveld Domain is a north-northwest elongated domain located between the Bushveld Complex's eastern and western lobes [35]. The Waterberg Group's primary

outcrop sites (Waterberg Plateau) are located between the Zoetfontein Fault and the Thabazimbi-Murchison Lineament, with two smaller outcrop areas to the west of Kanye in eastern Botswana [36]. The Nylstroom Syncline outcrop areas to the west of the Waterberg Plateau, as well as the Middleburg area, are part of the Central Bushveld Complex domain (Figure 2). Between Middelburg and Nylstroom, erosional outliers such as the Rust de Winter, Loskop, and Glentig Formations exist [37].

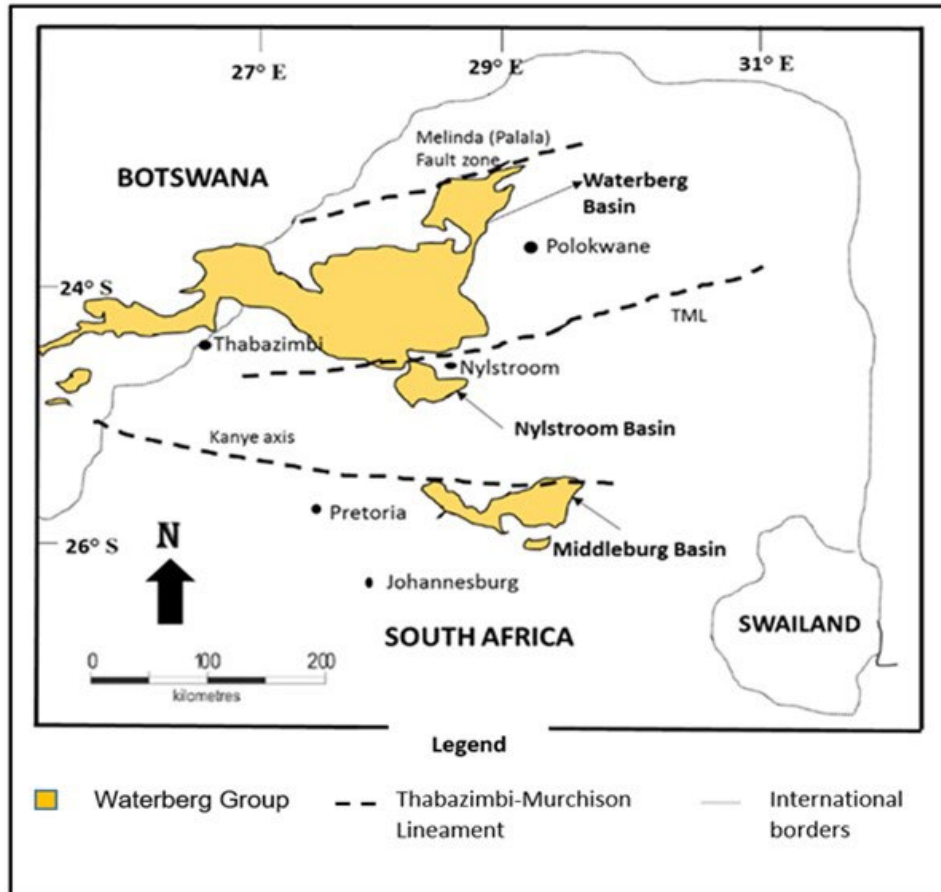


Figure 2. Geological map of the Waterberg Group (after [39])

The Waterberg Group is stratigraphically divided as shown in Figure 3. There are three basins in the Waterberg Group: the main Waterberg Basin, the Nylstroom Basin, and the Middleburg Basin (Figure 2). The Nylstroom, Matlabas, and Kransberg Subgroups are among the eleven formations that make up the main Waterberg Basin [2]. This research is focused on the Nylstroom Basin, which is made up of only two formations, the Swaershoek and Alma Formations. The Wilge River Formation is the sole formation found in the Middleburg Basin. The Glentig Formation is an unconformity-bounded unit that is overlain by the Waterberg Group's Swaershoek Formation and underlain by the Rooiberg Group's Schrikkloof Formation (Figure 3). The Glentig Formation was deposited between the last magmatism of the Bushveld Complex and the deposition of the Late Paleoproterozoic red beds of the Waterberg Group [38]. The Glentig Formation is composed of reddish to purple shale at the base, followed by sandstone and lava. The upper section is made up of conglomerate with pebbles of lava, then chert, sandstone, quartzite, and grey quartz-feldspar porphyry. The age of the Waterberg Group is reviewed by [32] and can be constrained between  $2054 \pm 4$  Ma, the age of a quartz porphyry lava near the base of the Swaershoek Formation [32], and  $\sim 1.88$  to  $\sim 1.87$  Ga, the oldest precise ages from dolerite sills intruding the Waterberg Group.

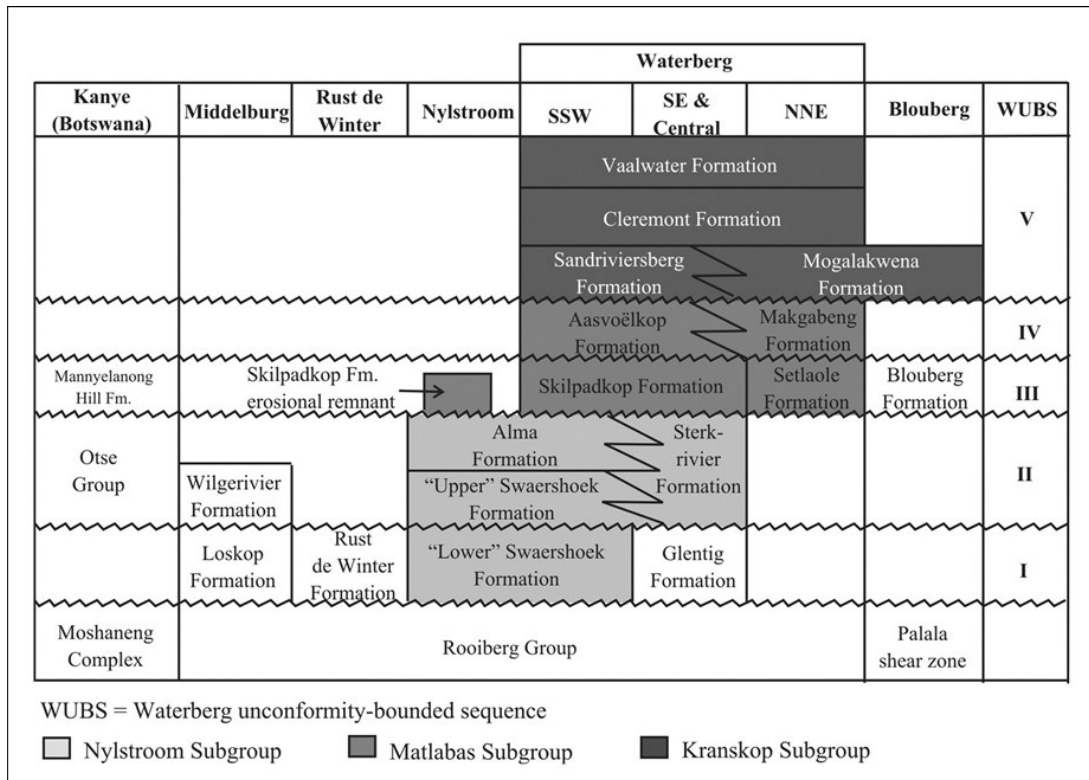


Figure 3. Stratigraphical subdivision of the Waterberg Group [32]

An unconformity-bounded unit is a unit of rocks that is bounded above and below designated discontinuities in the stratigraphic succession, preferably of regional or inter-regional extent [40]. The basic unconformity-bounded units are known as synthem [41], and their names are derived from their geographical location. These synthem are regional units separated by major unconformities, whether they are lithologically homogeneous or heterogeneous [41]. The units that are unconformity-bound are always diachronous [42]. According to [41], the nature of the bounding unconformities should be recognized to the extent that they overlap each other. Furthermore, the bounding unconformities must be extensive and distinguishable in order to be considered the boundaries of an unconformity-bounded unit. Likewise, [2] reported that an angular unconformity separates the upper contact of the Glentig Formation and the lower part of the Swaershoek Formation (Waterberg Group).

In the Nylstroom Basin, the Swaershoek Formation lies unconformably on top of the Glentig Formation [34]. It is made up of arenites and rudites with lutite intercalations and attained a maximum thickness of about 2500 m [41]. The Swaershoek Formation is divided into upper and lower parts (Figure 3), with the lower parts thought to have been deposited immediately after the Bushveld granites were deposited [43]. According to [44], the Swaershoek Formation conformably overlies the Rooiberg Group in the Modimolle (Nylstroom) area. Cheney and Twist [29] correlates the lower part of the Swaershoek Formation with the Loskop Formation, Rust de Winter Formation, and Glentig Formation. According to [44], the Swaershoek Formation is primarily composed of reddish sandstone, with minor interactions of conglomerate, purple and reddish-brown shale, and red amygdaloidal lava (Figure 2). Furthermore, the rudites contain pebbles to boulders of rhyolite, arenite, quartz vein, chert, iron-formation, jasper, rudite, and lutites [43]. The Alma Formation is composed primarily of sandstones and it lies beneath the Swaershoek Formation. In the Nylstroom Basin, the formation reaches a maximum thickness of approximately 1800 m [33]. The depositional environment of the Alma Formation is thought to be a combination of alluvial fans that form a bajada along a scarp caused by an uplifted block in the southern parts of the Murchison strike-slip fault zone [33].

### 3. Materials and methods

A geological investigation was carried out in the Glentig, Magalakynsoog, Geelhoutkloof, Vlakfontein, and Gembokfontein farms, north of Modimolle town (previously known as Nylstroom), where the Glentig, Swaershoek, and Alma Formations outcrop. The only outcrop of the Glentig Formation in South Africa is located in the Glentig farm, in the Limpopo Province, between longitudes 28°25'58.12" E and 28°29'22.13" E and latitudes 24°28'04.89" S and 24°26'05.33" S (Figure 1). The outcrops were studied in order to delineate and classify the various lithologies. During the field investigation, 38 representative sandstone samples were collected for petrographic and x-ray fluorescence analyses. A total of 76 sandstone thin sections were prepared (2 thin sections per sample) and analysed using a Nikon Lv-UEPI-N petrographic light microscope. The major and trace element geochemistry of the rocks was determined by X-ray fluorescence analysis (XRF) at the Department of Geology and Mining, University of Limpopo. The collected samples were crushed and milled, wherein 12 g of the sample was taken in for whole-rock XRF analysis. The crushed samples were milled for approximately 3 minutes in order to achieve a homogenous texture. Before using the milling machine for all the samples, the milling machine was cleaned of residual sample dust using ethanol to avoid contamination of samples. The milled samples were roasted at 1000 °C for a period of at least 3 hours to oxidize sulphur (S) and ferrous ion (Fe<sup>2+</sup>) in order to determine the loss of ignition (LOI). Thereafter, the powdered sample of approximately 12 g was mixed with a 3 g of cellulose binder using a pestle and mortar. Then, the 15 g powdered mixture was pressed using a hydraulic press at 20 to 25 T pressure in order to produce a homogenous pellet. The pressed pellets were labelled and ran through an Epsilon 3XLE EDXRF spectrometer, which has a 50 kV mA high-performance ceramic tube. The Epsilon software program was used to quantify for the major and trace elements. The major elements that were analysed are SiO<sub>2</sub>, TiO<sub>2</sub>, Al<sub>2</sub>O<sub>3</sub>, Fe<sub>2</sub>O<sub>3</sub>, MnO, MgO, CaO, Na<sub>2</sub>O, K<sub>2</sub>O, P<sub>2</sub>O<sub>5</sub> and Cr<sub>2</sub>O<sub>3</sub>. The analysed trace elements are As, Ba, Ce, Co, Cr, Cu, Ga, Hf, La, Mo, Nb, Nd, Ni, Pb, Rb, Sc, Sn, Sr, Ta, Th, Tl, U, V, W, Y, Yb, Zn, and Zr. The data received from the software program were tabulated and plotted on binary and ternary diagrams for geochemical interpretation.

### 4. Results

#### 4.1. Field observations

The Swaershoek Formation is about 300 m thick and unconformably overlies the Rooiberg Group (Figure 4a). The base of the formation in the Yellowwood Game Lodge is a 90 m thick fine-to-medium-grained massive sandstone. Overlying the massive sandstone is a clast-supported, poorly to moderately well-sorted conglomerate. A quartz-feldspar porphyry overlies the clast-supported conglomerate, which is approximately 26 m thick (Figure 4b-d). The quartz-feldspar porphyry has a thickness of about 12 m. There were no chill margins observed on the conglomerate or sandstone, indicating that the quartz-feldspar-porphyry is possibly extrusive. The feldspar-quartz porphyry is overlain by a 36-m-thick layer of medium-grained, planar cross-bedded sandstone. This sandstone is overlain by a brownish, coarse-grained massive sandstone with a thickness of about 10 m in the Yellowwood lodge and it is characterized by the intrusion of multiple quartz veins.

In the Yellowwood Game Lodge, the Alma Formation rests conformably on the Swaershoek Formation (Figure 5). The Alma Formation outcrop can be seen at the Yellowwood Game Lodge and extends into the Magalakynsoog North Farm. The thickness of the formation measured in the aforementioned locations is approximately 190 m. The formation's bottom is composed of a brown to light pink medium-grained massive sandstone. The maximum thickness of the basal unit is approximately 27 m. The massive sandstone and the underlying rhyodacite have a sharp contact (Schrikkloof Formation in the Rooiberg Group). A 13-meter-thick matrix-supported conglomerate overlies the massive sandstone. Quartzite, lava, and sand-size particles make up the polymictic pebble conglomerate. The clasts range from subrounded to well-rounded. The conglomerate matrix is composed of the same fine-to-medium-grained massive sandstone. The unit reaches a maximum thickness of about 11 m in the Magalakynsoog North Farm.



Figure 4. Photographs of the Swaershoek Formation showing: (a) Swaersberg mountain; (b) Quartz-feldspar porphyry; (c) massive sandstone; (d) Clast supported conglomerate; (e) matrix-supported cobble conglomerate with clast supported cobble conglomerate towards the top right of the image; (f) Cobble conglomerate truncated by quartz veins, the top part- the clast conglomerate grades to a matrix-supported conglomerate; (g) Conglomerate with lenses of coarse-grained sandstone (The red lines indicate the location of the sandstones lenses within the conglomerate); (h) Clast supported conglomerate truncated by an east-west striking blocky quartz vein

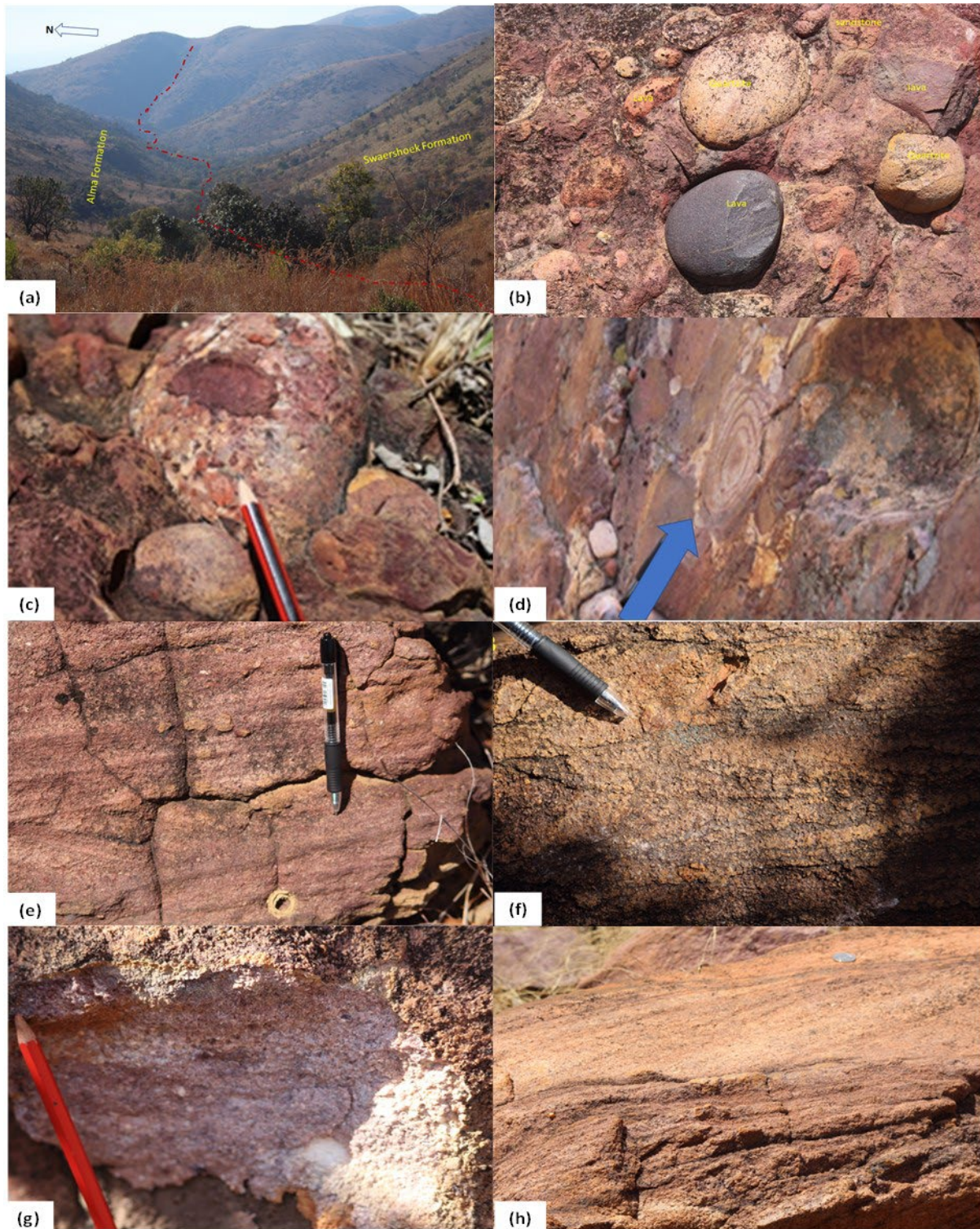


Figure 5. Photographs of the Alma Formation showing: (a) the contact between the Alma and Swaershoek Formations; (b) Polymictic cobble conglomerate; (c) Conglomerate clast which has in turn pebbles of quartzite and lava; (d) Spherical weathering of clasts; (e) Planar bedded sandstone; (f-g) Trough cross-bedded sandstone; (h) Planar bedded sandstone

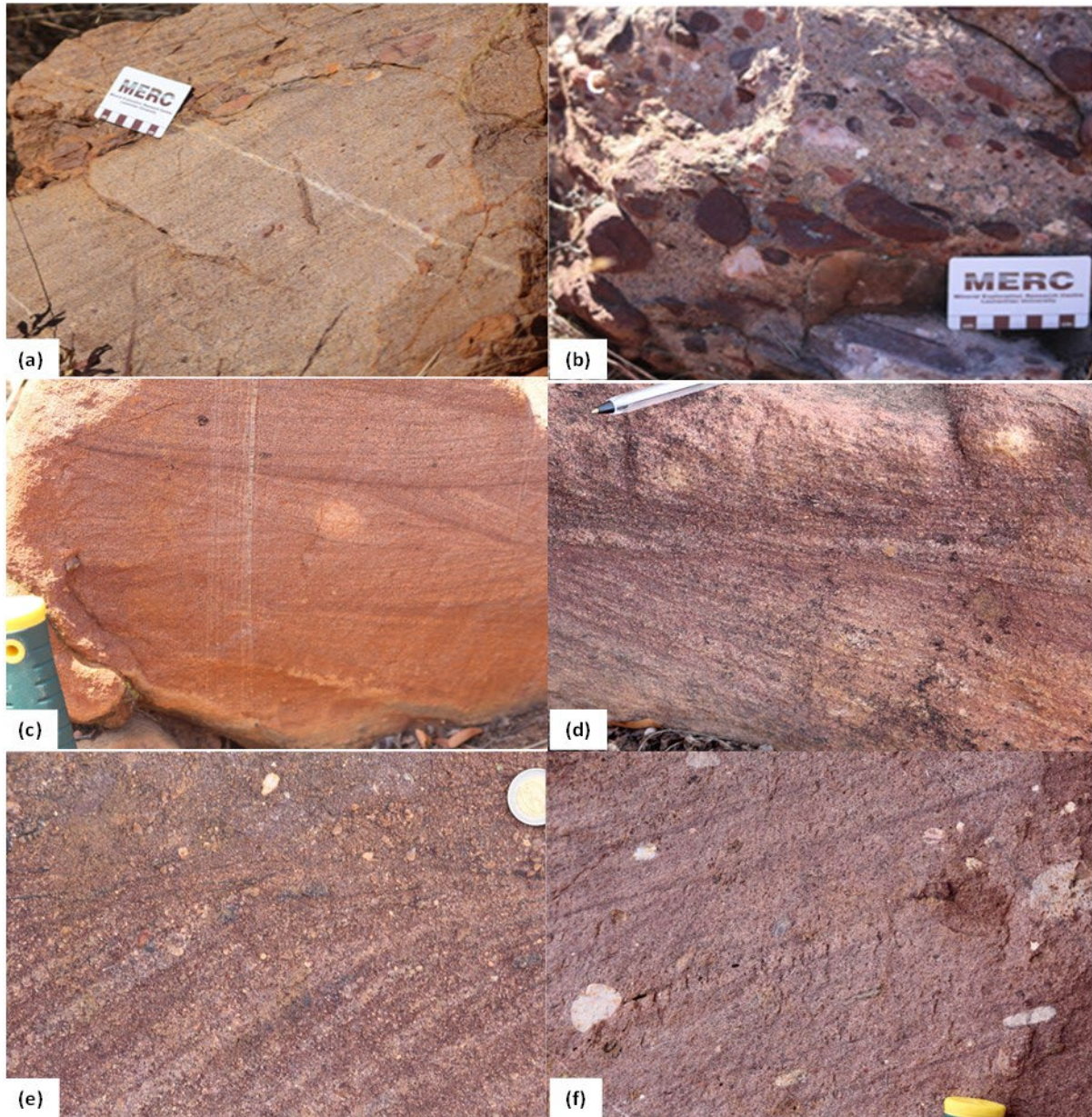


Figure 6. Photographs of the Glentig Formation showing: (a) Faint horizontally laminated sandstone; (b) Matrix supported sandstone; (c) Low angle trough cross-bedded sandstone; (d) Trough cross-bedded sandstone; (e) Cross-bedded sandstone with occasional pebbles of quartz; (f) Planar bedded sandstone with occasional pebbles of quartzite

The transition from a pebble conglomerate to a cobble conglomerate is marked by a gradational contact. The cobble conglomerate is a polymictic conglomerate supported by clasts. The majority of the clasts are boulders with diameters greater than 256 mm. The larger clasts are quartzite, while the smaller clasts are sandstones. The cobble conglomerate is overlain by a massive sandstone. The massive sandstone ranges in colour from brown to light pink and has a thickness of approximately 87 m. Overlying the massive sandstone is a cobble-sized oligomictic conglomerate. The conglomerate clasts are quartzite and range in diameter from 158 mm to 260 mm. The matrix is made up of fine- to medium-grained sandstone.

The Glentig Formation rests unconformably on the Rooiberg Group. It has a small area because it is confined to the south-eastern edge of the Yellowwood Game Lodge on the Swaersberg mountain slopes (Figure 1). The Glentig Formation is a 400 m thick succession of

sandstones topped by a thick grey quartz-feldspar porphyry. The Glentig Formation's lower unit is made up of planar-bedded sandstone with minor siltstone intercalation. The lower unit is approximately 100 m thick from the base and is overlain by cobble-sized conglomerate. Gradational contact exists between the underlying sandstone and the cobble-sized conglomerate. The conglomerate's clasts are mostly quartzite cobbles and lava, with a medium-to-coarse-grained sandstone matrix (Figure 6). In the Magalakynsoog North Farm, the conglomerate reached a maximum thickness of about 100 m. A greyish quartz-feldspar porphyry lies on top of the cobble conglomerate. In the study area, the porphyry reaches a maximum thickness of about 200 m. The porphyry trends east to west and thins towards the edges of the Glentig Formation in the east, reaching maximum thickness on the formation's western side. The stratigraphic section of the Alma, Swaershoek and Glentig Formations in both Yellowwood Game Lodge and Magalakynsoog North Farm is shown in Figure 7.

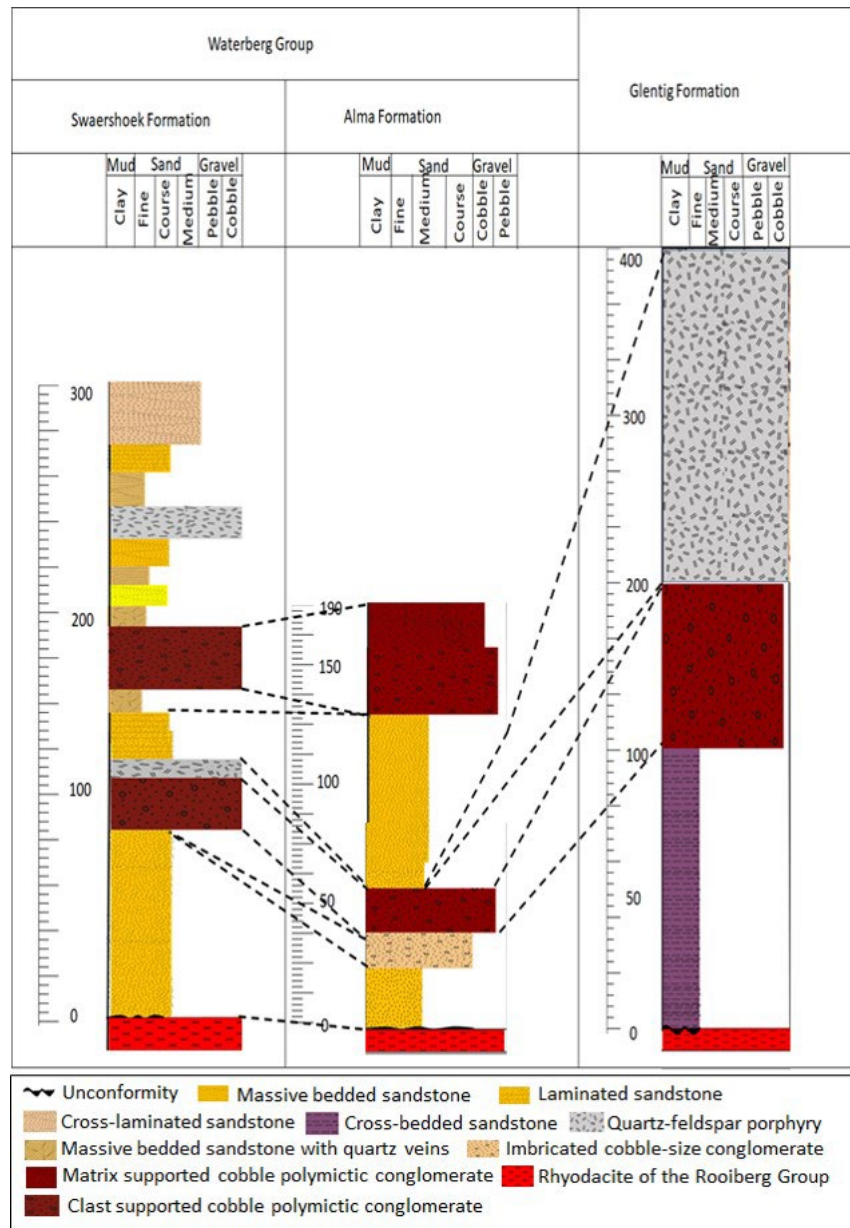


Figure 7. Stratigraphic correlation of the Swaershoek, Alma and Glentig Formations

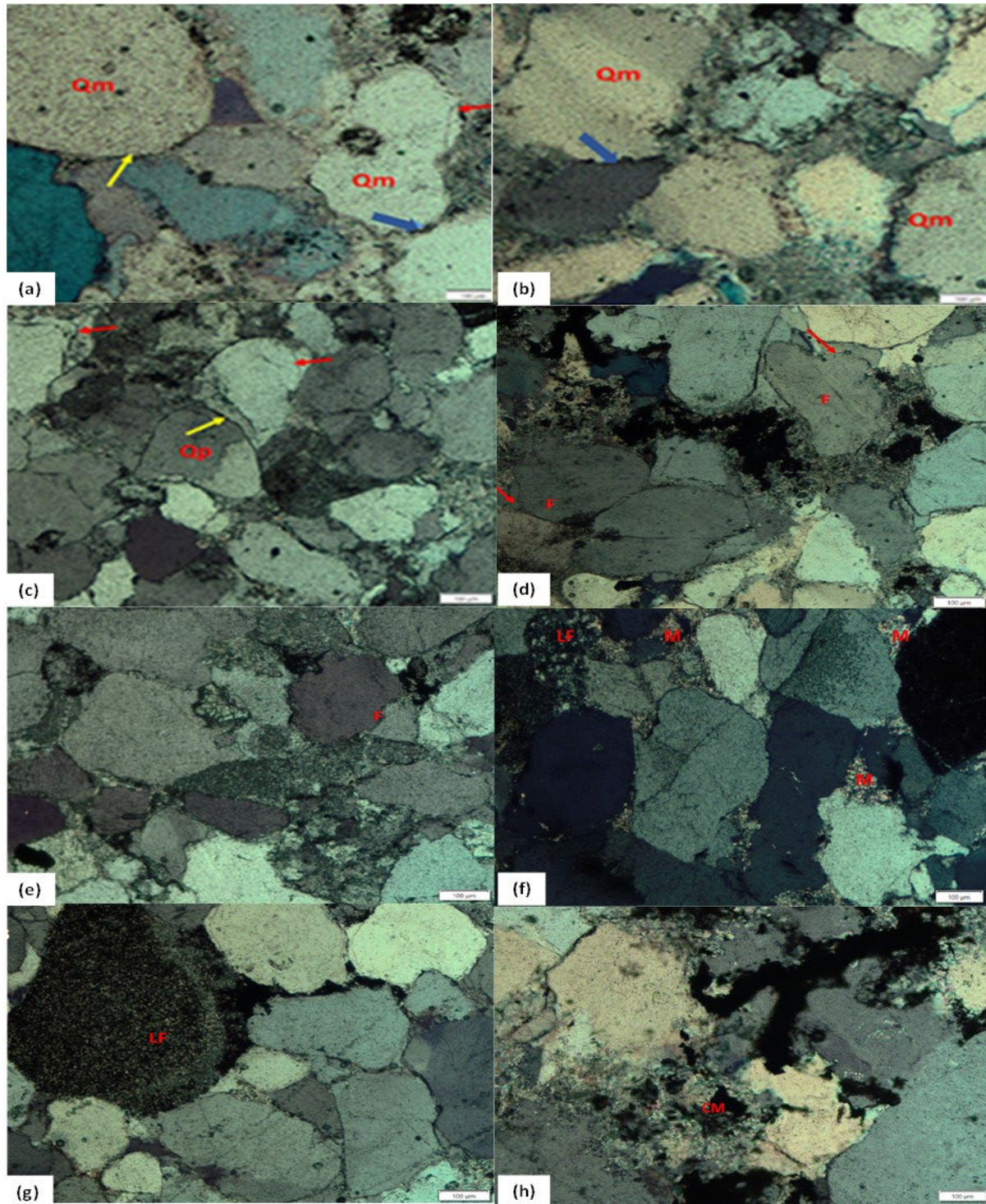


Figure 8. Photomicrographs showing: (a-c) Monocrystalline quartz (Qm) and polycrystalline quartz (Qp), and quartz overgrowth in the sandstones of the Swaershoek Formation; (c-e) Feldspar (F), feldspar overgrowth and replacement of feldspar by replaced by clay minerals; in the sandstones of the Alma Formation; (f-h) Quartz, feldspar, clay minerals, mica (M) and lithic fragments (LF) in the sandstones of the Glentig Formation

## 4.2. Sandstone petrography

Quartz is the most dominant mineral found in the samples. It usually appears colourless and it is less weathered compared to other minerals. The mineral commonly occurs as a monocrystalline quartz and a few occurring as polycrystalline quartz. Both alkali feldspar (orthoclase) and plagioclase feldspar (albite) are present in the thin sections, with alkali feldspar being the most dominant. These feldspars are much easily weathered compared to quartz minerals. In addition, the feldspar grains are smaller in size and less rounded when compared to the quartz grains. Just like the quartz grains, both monocrystalline and polycrystalline feldspar grains are present and there are feldspar overgrowths. Occasionally, there is present of reddish-brown stain, perhaps hematite rims around the original detrital feldspar grain. Some of the feldspar grains partially replaced or altered by clay minerals. The identified rock fragments are sedimentary, and these shards of rock have been weathered to sand-size particles and are now sand grains in the sedimentary rock (Figure 8). The framework grains are bound together by both the matrix and cement. The matrix is mostly clay minerals and they are either detrital or diagenetic in form. The common cementing minerals are clay, quartz overgrowth, and feldspar overgrowth. The mica in the sandstones is muscovite and biotite, with muscovite occurring more frequently than biotite. The mica is found as clasts and as matrix.

## 4.3. Sandstone geochemistry

### 4.3.1. Major elements

The result of the major elements analysis is presented in Table 1. The result shows that the concentration of SiO<sub>2</sub> or silica range is wide in all the samples, ranging from 31% to 97% with an average of 71%. There is a moderate concentration of Al<sub>2</sub>O<sub>3</sub> and Fe<sub>2</sub>O<sub>3</sub>, ranging from 2.3% to 26% and 0.4% to 16%, with an average of 10% and 5.6%, respectively. The concentration of TiO<sub>2</sub>, MnO, MgO, CaO, Na<sub>2</sub>O, K<sub>2</sub>O, P<sub>2</sub>O<sub>5</sub> and Cr<sub>2</sub>O<sub>3</sub> are low, ranging from 0.11% to 1.79%, 0.01% to 0.25%, 0.04% to 3.66%, 0.01% to 1.25%, 0.00% to 0.40%, 0.48% to 6.67%, 0.01% to 1.28% and 0.008% to 0.058%, respectively. In addition, TiO<sub>2</sub>, MnO, MgO, CaO, Na<sub>2</sub>O, K<sub>2</sub>O, P<sub>2</sub>O<sub>5</sub> and Cr<sub>2</sub>O<sub>3</sub> have an average concentration of 0.46%, 0.04%, 0.47%, 0.18%, 0.08%, 3.19%, 0.20% and 0.03% respectively. Al<sub>2</sub>O<sub>3</sub> is inert and that is why it is less mobile unlike other oxides; hence its abundance was used to compare with other oxides. The detected major oxides in the analysed samples were plotted against Al<sub>2</sub>O<sub>3</sub>, to compare their mobility to Al<sub>2</sub>O<sub>3</sub> (Figure 9). The Al<sub>2</sub>O<sub>3</sub> shows a positive correlation with MgO and Fe<sub>2</sub>O<sub>3</sub>, whereas TiO<sub>2</sub>, CaO, Na<sub>2</sub>O, and P<sub>2</sub>O<sub>5</sub> shows no trend. The positive correlation of MgO and Fe<sub>2</sub>O<sub>3</sub> with Al<sub>2</sub>O<sub>3</sub> perhaps suggests that they are associated with micaceous/clay minerals.

In the binary plot variation diagram of major elements against SiO<sub>2</sub> (Figure 10), MgO, TiO<sub>2</sub>, Al<sub>2</sub>O<sub>3</sub> and Fe<sub>2</sub>O<sub>3</sub> show a negative correlation to SiO<sub>2</sub>, while there is no trend for the other major elements. The increase in SiO<sub>2</sub> marks a maturity in the sandstone, resulting in a decrease of feldspars and volcanic rock fragments. The negative correlation of SiO<sub>2</sub> with the other major elements is attributable to most of the silica being sequestered in quartz. Also, the samples were normalised to UCC, PAAS and NASC (Figures 11 – 13; Table 2). Most samples from the Glentig, Alma and Swaershoek Formations are lower as compared to the UCC and NASC concentrations. However, two samples from the Swaershoek Formation shows a positive correlation and enrichment of P<sub>2</sub>O<sub>5</sub>. The other samples in the contextual information showed the values that were close to that of the NASC and almost the same values or concentrations of potassium feldspar (Figure 9). The Fe<sub>2</sub>O<sub>3</sub> content, though slightly lower in one sample from the Alma Formation, most of the recorded concentrations are similar to those of NASC and UCC. The Spider plot of major elements normalized against UCC shows a depletion of CaO in all the samples (Figure 12). However, there is a slight increase in the enrichment of potassium feldspar, which could be attributed to the presence of potassium-rich rocks around the area or from the source area. Generally, the concentrations of CaO in the analysed samples are comparable to or the same as the concentrations of the PAAS and the NASC (Figure 12). The plot of major elements shows a slight enrichment of Fe<sub>2</sub>O<sub>3</sub>, which is consistent with previous

plots. Samples from Glentig Formation also shows a slight depletion of MgO (Figure 13). Only one sample from the Swaershoek Formation exhibits depletion in the concentration of TiO<sub>2</sub>.

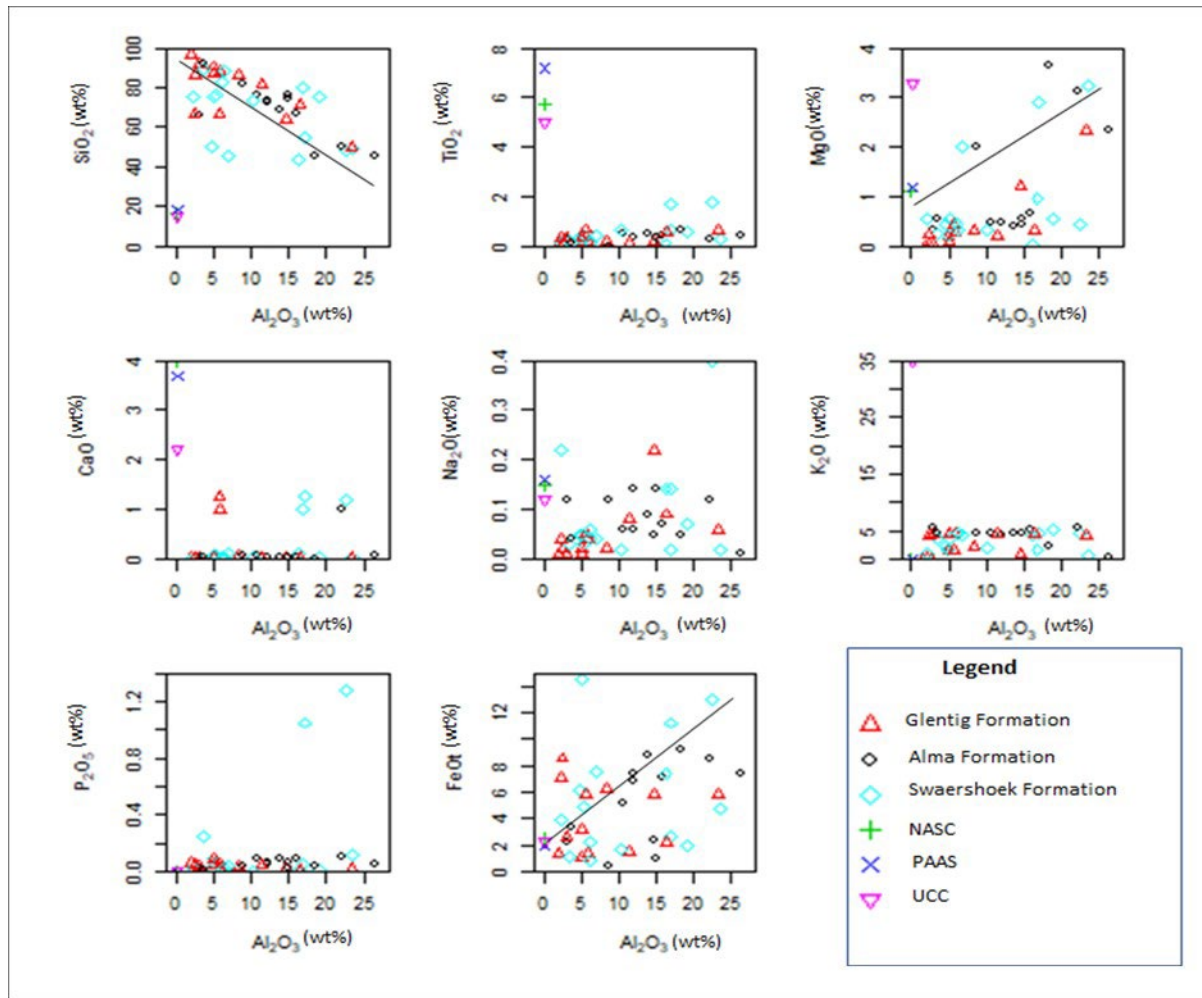


Figure 9. Binary plot of major elements versus Al<sub>2</sub>O<sub>3</sub> showing the distribution of samples from Glentig, Alma and Swaershoek Formations [15]. The average UCC, PAAS and NASC data were included for comparison

Table 1. Results of major oxide compositions (wt%) analysed by X-ray fluorescence spectrometry

Formation	Lithology	Sample ID	SiO <sub>2</sub>	TiO <sub>2</sub>	Al <sub>2</sub> O <sub>3</sub>	Fe <sub>2</sub> O <sub>3</sub>	MnO	MgO	CaO	Na <sub>2</sub> O	K <sub>2</sub> O	P <sub>2</sub> O <sub>5</sub>	Cr <sub>2</sub> O <sub>3</sub>	LOI
Alma	Sandstone	PEB 001	86.61	0.12	2.45	9.5	0.02	0.04	0.03	0.02	0.68	0.046	0.113	0.46
Alma	Sandstone	PEB 002	72.55	0.38	12.05	8.28	0.05	0.48	0.04	0.06	4.17	0.056	0.022	1.89
Alma	Sandstone	PEB 003	73.34	0.34	12	7.64	0.05	0.47	0.04	0.14	4.16	0.063	0.008	1.71
Alma	Sandstone	PEB 004	67.03	0.46	15.88	7.85	0.05	0.66	0.03	0.07	5.13	0.096	0.009	2.78
Alma	Sandstone	PEB 005	90.4	0.19	4.96	1.21	0.02	0.19	0.02	0.02	1.65	0.051	0.058	0.73
Alma	Sandstone	PEB 006	96.23	0.11	1.88	1.5	0.01	0	0.03	0.01	0.48	0.061	0.057	0.27
Alma	Sandstone	PEB 007	75.71	0.09	4.96	16.15	0.03	0.23	0.09	0.05	1.64	0.093	0.018	0.67
Alma	Sandstone	PEB008	66.3	0.33	3.02	2.56	0.01	0.33	0.04	0.12	5.66	0.025	0.112	2.18
Alma	Sandstone	PEB009	75.9	0.45	5.22	5.41	0.05	0.55	0.08	0.03	3.66	0.052	0.253	0.82
Alma	Sandstone	PEB010	86.36	0.23	8.33	6.88	0.02	0.32	0.06	0.02	2.11	0.036	0.005	1.58
Alma	Sandstone	PEB011	75.32	0.12	2.22	4.33	0.03	0.56	0.02	0.22	0.88	0.023	0.026	3.32
Alma	Sandstone	PEB012	50.21	0.36	4.66	6.88	0.01	0.45	0.03	0.05	2.32	0.024	0.034	3.23
Alma	Sandstone	PEB013	45.66	0.45	6.88	8.32	0.04	2.01	0.12	0.04	4.16	0.035	0.045	0.47
Alma	Sandstone	PEB 016	68.62	0.5	13.75	9.8	0.04	0.42	0.03	0.09	4.59	0.093	0.011	2.18
Glentig	Sandstone	MEL0012	88.32	0.2	5.86	1.54	0.02	0.27	1	0.04	4.59	0.046	0.015	0.82

Formation	Lithology	Sample ID	SiO <sub>2</sub>	TiO <sub>2</sub>	Al <sub>2</sub> O <sub>3</sub>	Fe <sub>2</sub> O <sub>3</sub>	MnO	MgO	CaO	Na <sub>2</sub> O	K <sub>2</sub> O	P <sub>2</sub> O <sub>5</sub>	Cr <sub>2</sub> O <sub>3</sub>	LOI
Glentig	Sandstone	MEL0015	76.63	0.5	10.66	5.73	0.05	0.5	0.07	0.06	4.59	0.094	0.022	1.58
Glentig	Sandstone	MEL0016	54.64	1.68	17.04	12.5	0.25	2.91	1.25	0.14	4.59	1.05	0.025	3.32
Glentig	Sandstone	MEL0017	47.95	1.79	22.56	14.4	0.06	0.46	1.2	0.4	4.59	1.28	0.019	3.23
Glentig	Sandstone	MEL0018	91.92	0.35	3.01	2.96	0.01	0.04	0.01	0.01	4.59	0.042	0.037	0.47
Glentig	Sandstone	MEL026	74.25	0.13	14.82	2.68	0.04	0.45	0.04	0.05	4.59	0.061	0.011	2.16
Glentig	Sandstone	MELS0016	87.22	0.35	5.01	3.54	0.03	0.1	0.02	0.01	4.59	0.085	0.018	0.9
Glentig	Sandstone	MEL0025	81.36	0.11	11.43	1.61	0.01	0.22	0.01	0.08	4.59	0.048	0.008	1.76
Glentig	Sandstone	MEL0019	49.66	0.32	23.54	5.33	0.02	3.22	0.02	0.02	0.68	0.113	0.046	2.18
Glentig	Sandstone	MEL0020	50.21	0.65	23.33	6.44	0.01	2.33	0.03	0.06	4.17	0.022	0.056	0.82
Glentig	Sandstone	MEL0021	43.88	0.11	16.24	8.21	0.03	0.05	0.12	0.14	4.16	0.008	0.063	1.58
Glentig	Sandstone	MEL0022	75.65	0.58	19.04	2.12	0.04	0.54	0.03	0.07	5.13	0.009	0.096	3.32
Glentig	Sandstone	MEL0023	80.36	0.69	16.88	3.01	0.06	0.98	1.02	0.02	1.65	0.058	0.051	3.23
Glentig	Sandstone	MEL0024	45.75	0.47	26.44	8.21	0.01	2.33	0.07	0.01	0.48	0.057	0.061	0.47
Swaer-shoek	Sandstone	MEL0026	66.63	0.68	5.66	6.44	0.03	0.45	1.25	0.05	1.64	0.018	0.093	2.18
Swaer-shoek	Sandstone	MEL0027	50.65	0.26	22.21	9.44	0.05	3.11	1.02	0.12	5.66	0.112	0.025	0.82
Swaer-shoek	Sandstone	MEL0028	89.21	0.23	3.44	1.25	0.06	0.25	0.01	0.03	3.66	0.253	0.052	1.58
Swaer-shoek	Sandstone	MEL0029	73.44	0.66	10.21	1.88	0.02	0.33	0.04	0.02	2.11	0.005	0.036	3.32
Swaer-shoek	Sandstone	MEL0030	63.88	0.21	14.66	6.44	0.04	1.22	0.02	0.22	0.88	0.026	0.023	3.23
Swaer-shoek	Sandstone	MEL0031	45.36	0.65	18.36	10.22	0.06	3.66	0.01	0.05	2.32	0.034	0.024	0.47
Swaer-shoek	Sandstone	MEL0032	66.32	0.32	2.33	7.88	0.03	0.23	0.03	0.04	4.16	0.045	0.035	2.16
Swaer-shoek	Sandstone	MEL0033	71.63	0.54	16.44	2.44	0.04	0.33	0.04	0.09	4.59	0.011	0.093	0.9
Swaer-shoek	Sandstone	MEL0034	92.54	0.12	3.55	3.69	0.03	0.55	0.04	0.04	4.59	0.015	0.046	1.76
Swaer-shoek	Sandstone	MEL0035	88.36	0.14	6.22	2.55	0.02	0.32	0.03	0.06	4.59	0.022	0.094	0.46
Swaer-shoek	Sandstone	MEL0036	76.54	0.34	14.88	1.08	0.05	0.56	0.02	0.14	4.59	0.025	1.05	1.89
Swaer-shoek	Sandstone	MEL0037	83.22	0.12	6.11	1.01	0.06	0.45	0.03	0.04	4.59	0.019	1.28	1.71
Swaer-shoek	Sandstone	MEL0038	81.63	0.02	8.72	0.44	0.01	2.01	0.09	0.12	4.59	0.037	0.042	2.78
UCC			66.6	0.64	15.4	5.04	0.1	2.48	3.59	3.27	2.8	0.12		
PAAS			62.4	0.99	18.78	7.18	0.11	2.19	1.29	1.19	3.68	0.16		
NASC			64.82	0.8	17.05	5.7	0.1	2.83	3.51	1.13	3.97	0.15		

Table 2. Comparison of the average major elements composition of this study with those of the standard values

Oxide (wt.%)	This study (sandstone)	UCC	PAAS	NASC
SiO <sub>2</sub> (%)	71.40	66.6	62.40	64.82
TiO <sub>2</sub> (%)	0.40	0.64	0.99	0.80
Al <sub>2</sub> O <sub>3</sub> (%)	10.90	15.40	18.78	17.05
Fe <sub>2</sub> O <sub>3</sub> (%)	5.59	5.04	7.18	5.70
MnO (%)	0.04	0.10	0.11	0.00
MgO (%)	0.84	2.48	2.19	2.83
CaO (%)	0.20	3.59	1.29	3.51
Na <sub>2</sub> O (%)	0.07	3.27	1.19	1.13
K <sub>2</sub> O (%)	3.47	2.80	3.68	3.97
P <sub>2</sub> O <sub>5</sub> (%)	0.11	0.12	0.16	0.15

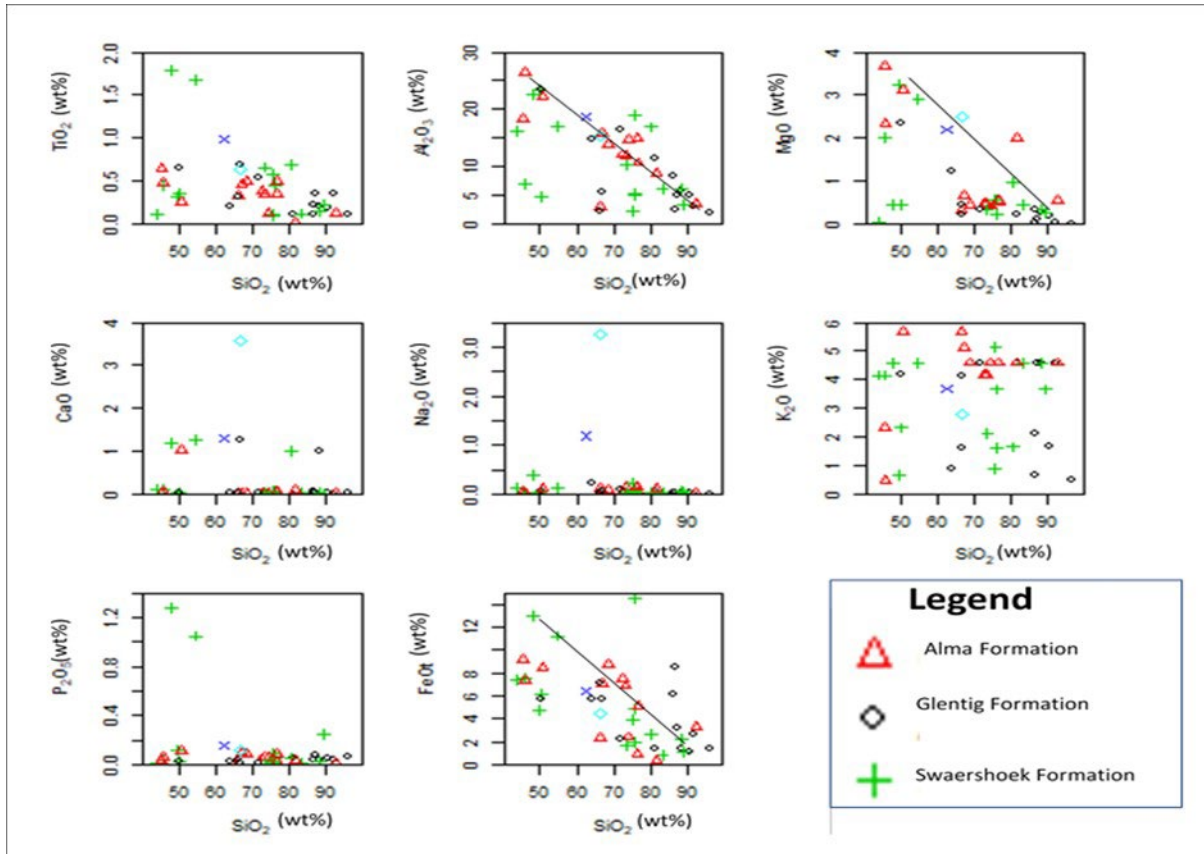


Figure 10. Binary plot of major elements against  $\text{SiO}_2$  variation diagrams for the Glentig, Alma and Swaershoek Formations

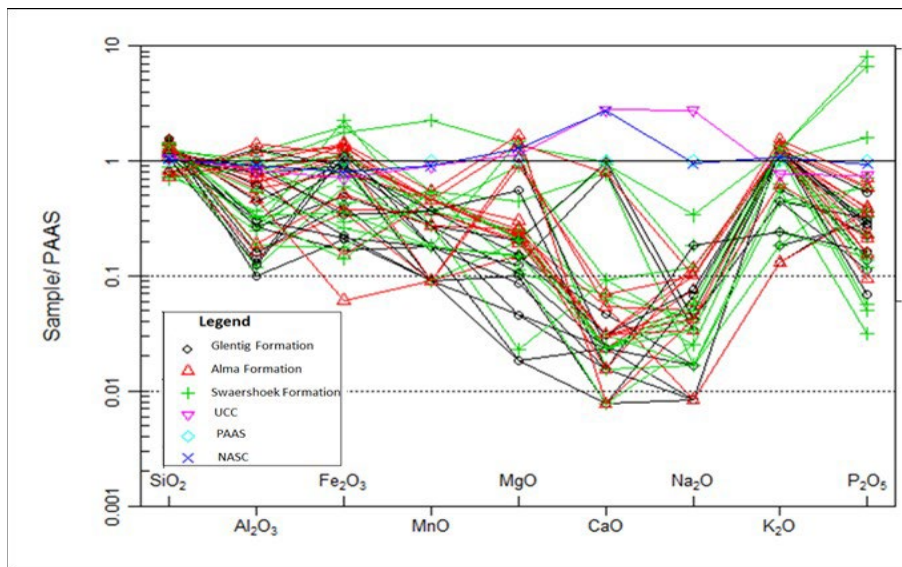


Figure 11. Spider plot of major elements normalised against PAAS (after [7,46])

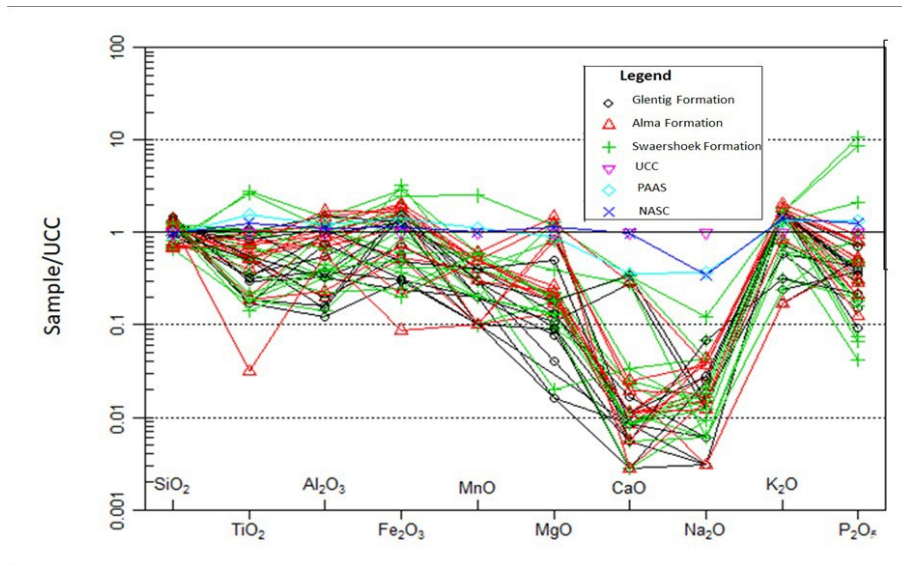


Figure 12. Spider plot of major elements normalised against UCC (after [7,46])

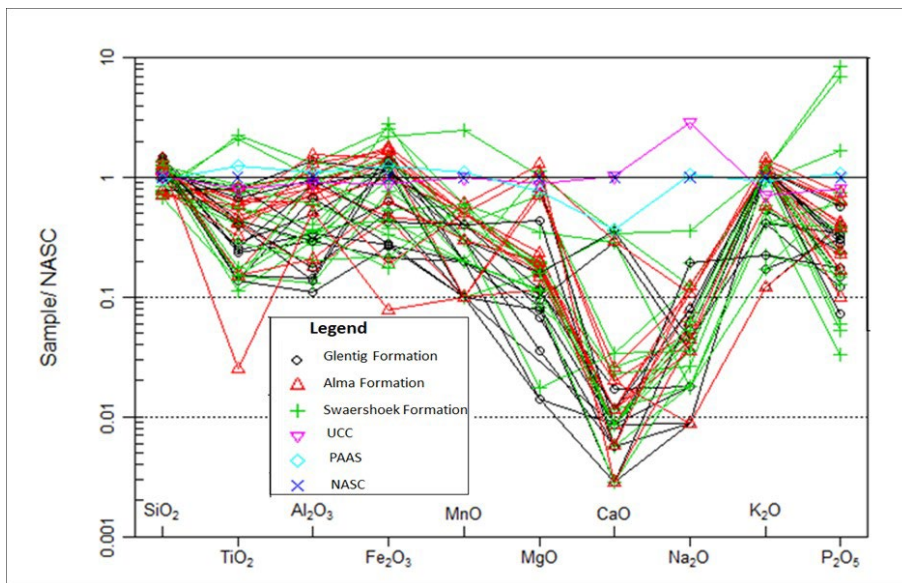


Figure 13. Spider plot of major elements normalised against NASC (after [7,46])

### 4.3.2. Trace elements

Trace elements concentration in the sandstones of the Glentig, Alma and Swaershoek Formations are presented in Table 3 (A-B). The trace element fields were grouped into large ion lithophile elements (LILE), high field strength elements (HFSE) and transition trace elements (TTE). The result shows that the concentration of LILE ranges from 2.80 to 3290 ppm for Ba, 2.01 to 618 ppm for Rb, 2.10 to 240 ppm for Sr, 1.18 to 216 ppm for Th, and 0.1 to 8.9 ppm for U. The concentration of the HFSE, such as Zr, Hf, Y and Nb, ranges from 82ppm to 596 ppm, 2.76 ppm to 14 ppm, 0.5 ppm to 146 ppm and 0.62 ppm to 65 ppm, respectively. The concentration of the TTE like Sc, V, Cr, Ni, and Zn varies from 0.3 ppm to 25 ppm, 0.07 ppm to 149 ppm and 8.6 ppm to 393 ppm, 0.27 ppm to 131 ppm and 0.09 ppm to 586 ppm, respectively. Just like the major elements, the concentrations of these trace elements are compared with the average concentration of those of UCC and PAAS. The concentration studied samples are generally comparable to those of UCC and PAAS (Figures 14-15). However, the spider plot of trace elements normalised against UCC (Figure 14) shows the depletion of

Rb, V and Zn. The LILE shows a depletion of Rb for Swaershoek Formation and slightly higher for samples from the Glentig and Alma Formations. The HFSE concentration shows depletion of Y, while an enrichment was recorded for Hf for the Glentig Formation.

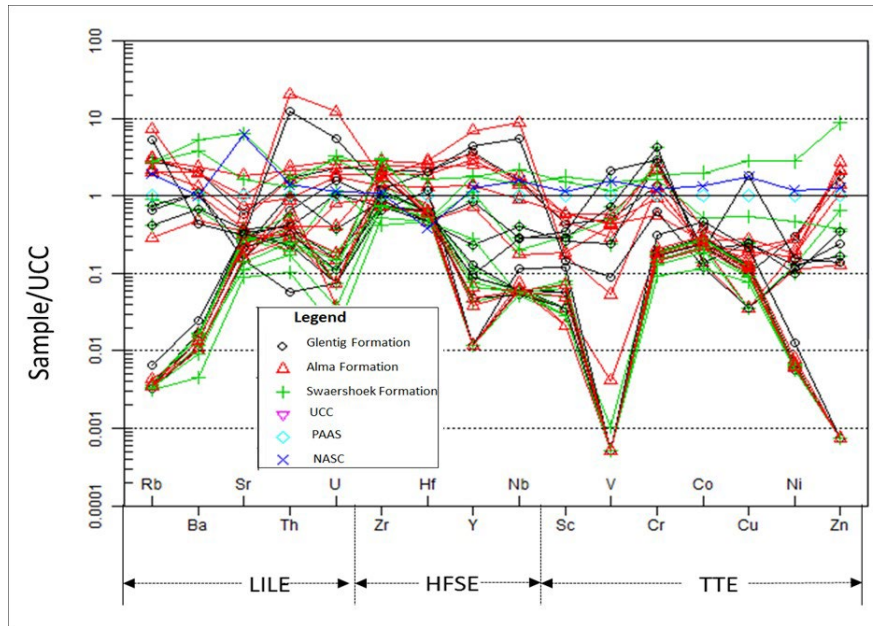


Figure 14. Spider plot of trace element normalised with UCC

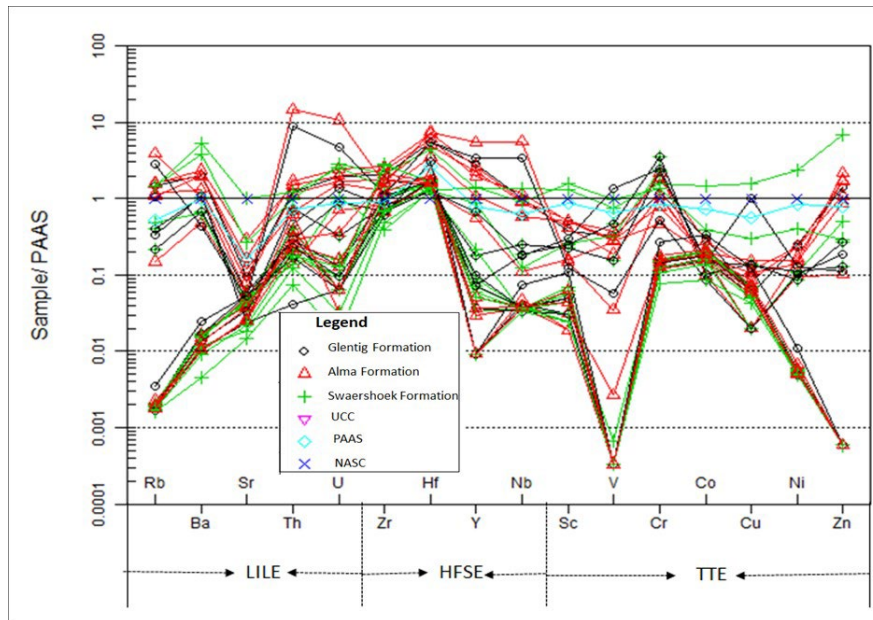


Figure 15. Spider plot of trace element normalised with PAAS

Table 3A. Results of trace element compositions (wt%) analysed by X-ray fluorescence spectrometry

Formation	Lithology	Sample ID	As	Ba	Ce	Co	Cr	Cu	Ga	Hf	La	Mo	Nb	Nd	Ni
Alma	S	PEB 001	68	1277	244	6,9	127	2,8	22	11	135	2,1	19	110	14
Alma	S	PEB 002	7,6	303	68	2,3	239	<2	2,7	<5	33	2,2	2,1	28	5,3
Alma	S	PEB 003	74	833	135	3,9	118	<2	18	10	93	2	17	73	9,2
Alma	S	PEB 004	31	1493	122	4,4	51	7,7	22	12	78	2,7	22	55	8,4

Formation	Lithology	Sample ID	As	Ba	Ce	Co	Cr	Cu	Ga	Hf	La	Mo	Nb	Nd	Ni
Alma	S	PEB 005	NA	NA	NA	NA	NA	NA	NA	NA	NA	NA	NA	NA	NA
Alma	S	PEB 006	NA	NA	NA	NA	NA	NA	NA	NA	NA	NA	NA	NA	NA
Alma	S	PEB 007	22	402	47	3,4	255	<2	8,5	<5	22	2,7	2,4	25	6
Alma	S	PEB008	25	1221	236	4	87	4,3	23	14	163	3	18	130	13
Alma	S	PEB009	4,3	671	49	3,4	253	6,7	6,9	<5	25	2	4,8	15	6,1
Alma	S	PEB010	10	1260	86	6,4	203	5,8	15	7	43	2,2	11	41	13
Alma	S	PEB011	28	2421	204	34	175	79	21	8,7	88	2,9	26	62	131
Alma	S	PEB012	11	3290	338	8,9	150	15	22	<5	137	2,8	17	113	22
Alma	S	PEB013	4,6	429	64	2,4	393	7	4,5	<5	36	<2	3,5	31	4,7
Alma	S	PEB 016	25	1221	236	4	87	4,3	23	14	163	3	18	130	13
Glentig	S	MEL 0012	4,3	671	49	3,4	253	6,7	6,9	<5	25	2	4,8	15	6,1
Glentig	S	MEL 0015	10	1260	86	6,4	203	5,8	15	7	43	2,2	11	41	13
Glentig	S	MEL 0016	28	2421	204	34	175	79	21	8,7	88	2,9	26	62	131
Glentig	S	MEL 0017	11	3290	338	8,9	150	15	22	<5	137	2,8	17	113	22
Glentig	S	MEL 0018	4,6	429	64	2,4	393	7	4,5	<5	36	<2	3,5	31	4,7
Glentig	S	MEL 026	41	657	364	3,8	117	5,4	35	15	226	<2	106	115	7,5
Glentig	S	MELS 0016	<3	694	54	3,4	266	51	6,5	<5	22	3,4	3,4	11	7,2
Glentig	S	MEL 0025	11	276	61	2	57	<2	21	11	22	<2	65	19	5,6
Glentig	S	MEL 0019	1,10	2,80	15,1	1,98	8,60	2,15	0,74	2,47	0,43	2,71	0,62	1,79	0,27
Glentig	S	MEL0020	4,50	10,30	39,4	4,75	17,40	3,50	0,88	3,44	0,55	3,46	0,77	2,17	0,32
Glentig	S	MEL0021	3,90	10,50	40	4,77	16,70	3,41	0,83	3,46	0,56	3,21	0,70	2,11	0,31
Glentig	S	MEL0022	5,80	10,30	39,7	4,70	17,30	3,57	0,82	3,41	0,56	3,29	0,70	2,05	0,30
Glentig	S	MEL0023	3,10	10,20	39,9	4,73	17,00	3,51	0,83	3,30	0,55	3,39	0,74	2,11	0,32
Glentig	S	MEL0024	3,70	10,50	41,5	4,80	17,70	3,45	0,77	3,43	0,57	3,31	0,70	2,05	0,32
Swaer-shoek	S	MEL0026	4,20	10,60	39,6	4,86	17,50	3,42	0,80	3,36	0,56	3,61	0,71	2,13	0,32
Swaer-shoek	S	MEL0027	3,30	9,60	39,4	4,62	17,30	3,37	0,80	3,33	0,56	3,26	0,74	2,18	0,31
Swaer-shoek	S	MEL0028	2,70	10,10	40,4	4,81	17,60	3,31	0,80	3,45	0,56	3,49	0,71	2,06	0,31
Swaer-shoek	S	MEL0029	2,40	9,70	37,6	4,62	16,60	3,22	0,84	3,27	0,52	3,31	0,67	2,03	0,30
Swaer-shoek	S	MEL0030	3,40	8,70	34	4,17	15,60	3,21	0,80	3,35	0,56	3,38	0,73	2,21	0,30
Swaer-shoek	S	MEL0031	2,90	6,30	33,6	5,03	19,40	3,74	0,97	4,11	0,67	4,01	0,90	2,60	0,37
Swaer-shoek	S	MEL0032	0,60	6,80	29,2	3,75	13,30	2,80	0,73	2,90	0,47	2,95	0,63	1,89	0,27
Swaer-shoek	S	MEL0033	2,40	15,40	65,9	7,84	29,20	6,15	1,40	6,17	1,02	6,32	1,40	4,11	0,60
Swaer-shoek	S	MEL0034	9,10	6,90	31	3,78	13,90	3,07	0,75	3,21	0,53	3,28	0,72	2,19	0,30
Swaer-shoek	S	MEL0035	1,80	7,30	30	3,68	13,90	2,59	0,70	2,82	0,47	2,92	0,63	1,88	0,27
Swaer-shoek	S	MEL0036	5,60	6,40	27,6	3,48	13,30	2,74	0,76	3,04	0,50	3,34	0,71	1,99	0,28
Swaer-shoek	S	MEL0037	2,60	5,80	25,7	3,14	11,80	2,50	0,66	2,76	0,47	2,89	0,69	2,03	0,28
Swaer-shoek	S	MEL0038	4,30	8,40	34,6	4,28	16,20	3,28	0,80	3,22	0,52	3,20	0,72	2,02	0,29
UCC				626,00		17,00	92,00	28,00	17,50	5,30			12,00		47,00
PAAS				628,00		23,00	110,00	50,00	20,00	2,00			19,00		55,00

S-sandstone;

Table 3B. Results of trace element compositions (wt%) analysed by X-ray fluorescence spectrometry

Formation	L*	Samples	Pb	Rb	Sc	Sn	Sr	Ta	Th	Tl	U	V	W	Y	Yb	Zn	Zr
Alma	S	PEB 001	35	236	6,1	5,3	19	<2	18	3	6,1	49	<5	78	5,2	121	421
Alma	S	PEB 002	19	24	2,6	<3	11	<2	2	2,4	2,2	41	11	15	<4	8,6	174
Alma	S	PEB 003	33	185	6,6	3,9	16	<2	17	<2	5,2	28	<5	61	5,3	146	365
Alma	S	PEB 004	61	248	8,2	5,9	59	4,2	22	<2	6,2	42	<5	53	<4	73	496
Alma	S	PEB 005	NA	NA	NA	NA	NA	NA	NA	NA	NA	NA	NA	NA	NA	NA	NA
Alma	S	PEB 006	NA	NA	NA	NA	NA	NA	NA	NA	NA	NA	NA	NA	NA	NA	NA
Alma	S	PEB 007	24	77	4,2	3,5	8,9	3,8	2	2,1	3,2	48	7,6	24	<4	43	82
Alma	S	PEB008	65	260	8,3	6,2	33	2,5	25	<2	7,6	43	<5	71	7,4	142	551
Alma	S	PEB009	8,7	64	3,6	<3	6,7	<2	11	<2	<2	23	13	4,9	<4	11	171
Alma	S	PEB010	47	171	8,2	<3	24	<2	10	<2	4,8	56	7,6	29	<4	93	267
Alma	S	PEB011	41	234	21	3,1	53	<2	14	<2	8,9	114	9,3	37	<4	586	441
Alma	S	PEB012	65	234	25	4,8	204	4,2	18	<2	7,9	149	<5	38	<4	25	294
Alma	S	PEB013	13	35	4	<3	12	<2	4,2	<2	2,8	70	7	18	<4	23	141
Alma	S	PEB016	65	260	8,3	6,2	33	2,5	25	<2	7,6	43	<5	71	7,4	142	551
Glentig	S	MEL0012	8,7	64	3,6	<3	6,7	<2	11	<2	<2	23	13	4,9	<4	11	171
Glentig	S	MEL0015	47	171	8,2	<3	24	<2	10	<2	4,8	56	7,6	29	<4	93	267
Glentig	S	MEL0016	41	234	21	3,1	53	<2	14	<2	8,9	114	9,3	37	<4	586	441
Glentig	S	MEL0017	65	234	25	4,8	204	4,2	18	<2	7,9	149	<5	38	<4	25	294
Glentig	S	MEL0018	13	35	4	<3	12	<2	4,2	<2	2,8	70	7	18	<4	23	141
Glentig	S	MEL026	23	618	2,4	17	12	8,3	216	4,2	33	5,2	6,4	146	22	184	335
Glentig	S	MELS0016	618	54	4,8	<3	4,7	<2	6,9	2,1	4,2	202	5	<4	<4	9,3	170
Glentig	S	MEL0025	12	453	2	9,1	10	7,1	128	<2	15	8,7	<5	93	13	16	234
Glentig	S	MEL0019	1,66	0,26	0,40	146,40	2,90	33,40	1,10	<0,1	<0,1	<0,1	<0,1	5,90	<0,01	<0,1	101,00
Glentig	S	MEL0020	2,09	0,32	0,50	65,60	9,70	85,00	4,50	<0,1	0,20	<0,1	<0,1	<0,5	<0,01	<0,1	200,00
Glentig	S	MEL0021	1,97	0,30	1,10	56,00	8,10	71,60	3,90	<0,1	0,20	<0,1	<0,1	0,90	<0,01	<0,1	145,00
Glentig	S	MEL0022	2,06	0,30	0,90	63,60	9,30	77,80	5,80	<0,1	0,20	<0,1	<0,1	2,40	<0,01	<0,1	223,00
Glentig	S	MEL0023	1,99	0,31	0,40	57,00	8,50	86,40	3,10	0,10	0,50	0,10	<0,1	<0,5	<0,01	<0,1	210,00
Glentig	S	MEL0024	2,01	0,31	0,50	50,00	7,80	83,50	3,70	0,10	0,50	0,40	<0,1	0,80	<0,01	<0,1	141,00
Swaer-shoek	S	MEL0026	2,02	0,32	0,80	64,00	10,70	79,80	4,20	<0,1	0,40	<0,1	<0,1	2,70	<0,01	<0,1	225,00
Swaer-shoek	S	MEL0027	2,04	0,31	0,30	62,90	10,10	80,00	3,30	<0,1	0,40	<0,1	<0,1	<0,5	<0,01	<0,1	440,00
Swaer-shoek	S	MEL0028	2,05	0,33	0,50	61,30	9,50	77,10	2,70	<0,1	0,30	<0,1	<0,1	1,90	<0,01	<0,1	566,00
Swaer-shoek	S	MEL0029	2,04	0,30	0,70	56,20	8,90	67,50	2,40	<0,1	0,30	<0,1	<0,1	1,60	<0,01	<0,1	596,00
Swaer-shoek	S	MEL0030	2,03	0,30	0,80	87,90	6,80	64,10	3,40	<0,1	0,30	<0,1	<0,1	1,90	0,01	<0,1	147,00
Swaer-shoek	S	MEL0031	2,31	0,36	0,30	69,50	5,20	104,50	2,90	<0,1	0,20	<0,1	<0,1	<0,5	<0,01	<0,1	258,00
Swaer-shoek	S	MEL0032	1,78	0,27	0,50	71,40	4,80	97,20	0,60	<0,1	0,20	<0,1	<0,1	1,00	<0,01	<0,1	365,00
Swaer-shoek	S	MEL0033	3,75	0,55	1,70	169,50	10,50	42,00	2,40	<0,1	0,20	<0,1	0,10	<0,5	<0,01	<0,1	125,00
Swaer-shoek	S	MEL0034	1,91	0,31	0,70	71,00	4,90	101,70	9,10	<0,1	0,10	<0,1	<0,1	1,40	<0,01	<0,1	142,00
Swaer-shoek	S	MEL0035	1,77	0,27	1,00	68,30	3,60	94,20	1,80	<0,1	0,10	<0,1	<0,1	<0,5	<0,01	<0,1	142,00
Swaer-shoek	S	MEL0036	1,82	0,29	1,00	70,10	5,10	96,60	5,60	<0,1	0,20	<0,1	<0,1	<0,5	<0,01	<0,1	364,00
Swaer-shoek	S	MEL0037	1,69	0,28	0,40	54,90	4,40	156,70	2,60	<0,1	0,40	<0,1	<0,1	1,40	<0,01	<0,1	146,00
Swaer-shoek	S	MEL0038	1,94	0,29	0,70	75,00	7,50	75,90	4,30	<0,1	1,10	<0,1	<0,1	1,00	<0,01	<0,1	368,00
UCC			17,00	84,00	14,00		32,00		10,50		2,70	97		21,00		67	193,00
PAAS			20,00	160,00	16,00		200,00		14,60		3,10	150		27,00		85	

L\*- lithology; S-sandstone;

## 5. Interpretations and discussion

### 5.1. Petrography and mineralogy

Petrographic analysis reveals that quartz dominates the Swaershoek, Alma, and Glentig Formations, followed by feldspar, clay minerals, mica, and lithic fragments. There is more monocrystalline quartz and less polycrystalline quartz. According to [47], polycrystalline quartz is dominant at first, but it is usually broken down into monocrystalline quartz. The presence of monocrystalline quartz in high concentrations indicates sediment maturity. The petrographic study of sandstones and conglomerates from the study area also revealed that they are moderately to well-sorted with mostly sub-rounded to rounded grains. The lack of significant petrographically distinct compositional variations in the sandstones may indicate that their source was homogeneous. As a result, the transportation distance from the source area was inferred to be relatively long. According to Folk's [48] genetic and empirical classification of quartz types, monocrystalline quartz grains are primarily plutonic, hydrothermal, and recycled sedimentary in origin, whereas polycrystalline quartz grains are recrystallized and stretched metamorphic types. The presence of more monocrystalline quartz grains indicates that the sediments were mostly derived from a granitic source [49]. As reported by [50], such grains could have formed as a result of disaggregation of the original polycrystalline quartz during high energy or long-distance transport from the metamorphic source. The presence of a few pure feldspar grain fragments in some of the sandstones suggests an igneous source, whereas the altered feldspar grains suggest a metamorphic source [49]. The presence of mica could be due to the fact that in the depositional environment, muscovite is more chemically stable than biotite. The identified rock fragments are sedimentary in nature, and they have been eroded down to sand size, becoming sand grains in the sedimentary rock.

### 5.2. Source rock provenance

The studied samples were also compared to the Upper Continental Crust (UCC), North American Shale Composite (NASC), and Post-Archean Australian Shale (PAAS) (Figure 9; Table 2). The major elements show variations in the analysed samples, but still comparable with the average composition of the UCC, PAAS, and NASC. The average concentration of Na<sub>2</sub>O in this study is low as compared to those of UCC, PAAS and NASC, this could be due to the low amounts of Na-rich plagioclase in all the samples. The average K<sub>2</sub>O/Na<sub>2</sub>O ratio is 46, this indicates that there is a relatively high alteration of the feldspars. [45] reported the average N<sub>2</sub>O for the Rooiberg Group to be just greater >1, which perhaps indicates the presence of albite that has been altered slightly. In this study, the average K<sub>2</sub>O/Na<sub>2</sub>O is greater than >5 which for albite represents a high degree of alteration. The K<sub>2</sub>O enrichment also suggests the presence of illite and sericite, which are further proof of high weathering of the feldspars. Likewise, K<sub>2</sub>O is higher as compared to that of UCC and is slightly lower as compared to that of PAAS and NASC. This could be due to the fact that K and Na are strongly removed or depleted during weathering. The MgO and CaO average concentration is lower as compared to those of NASC, UCC and PAAS.

The concentration of major elements analysed for this study was used to determine the source rock provenances. Folk [48] defined provenance as a term that has been used to include all factors involving the production or birth of sediments. The definition of provenance was further expanded to encompass all factors related to sediment production, with "specific reference to the composition of the parent rocks as well as the physiography and climate of the source area" [7,52]. In this study, provenance discriminant analysis was used to differentiate between the four major provenances (mafic igneous, intermediated, felsic igneous and quartzose sedimentary or recycled provenances) as proposed by [53]. The discriminant function plot infers that the sediments from the Swaershoek, Alma and Glentig Formations have been derived from felsic and intermediate igneous provenances (Figure 16). These sediments could have been derived from the whining stages of the emplacement of the Bushveld igneous complex. Similarly, the binary plot of TiO<sub>2</sub> vs Zr indicates that the samples were derived from

intermediate and felsic rocks (Figure 17). However, one sample from the Swaershoek Formation was the outlier that plotted in the mafic igneous rocks, this could suggest that some of the sediments were derived from the mafic layers of the Bushveld Igneous Complex. Likewise, the binary plots of  $TiO_2$  versus Ni revealed that the samples are mostly of acid or felsic provenance (Figure 18). The findings of this study agrees with the work conducted by [43], wherein [43] reported that the rocks of the studied geologic formations originate from the Transvaal Group.

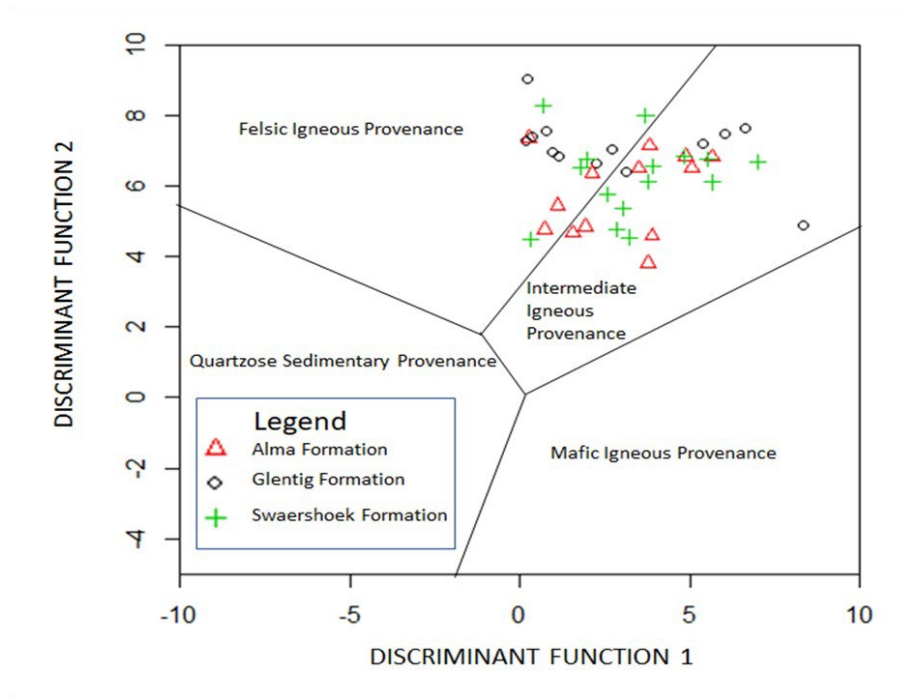


Figure 16. Major elements discrimination function diagram for the studies sandstones on the background diagram of [9] indicating the provenance of the source rocks. The discriminant functions are: Discriminant Function 1 =  $(-1.773 TiO_2) + (0.607 Al_2O_3) + (0.760 Fe_2O_3) + (-1.500 MgO) + (0.616 CaO) + (0.509 Na_2O) + (-1.224 K_2O) + (-9.090)$ ; Discriminant Function 2 =  $(0.445 TiO_2) + (0.070 Al_2O_3) + (-0.250 Fe_2O_3) + (-1.142 MgO) + (0.438 CaO) + (1.475 Na_2O) + (-1.426 K_2O) + (-6.861)$

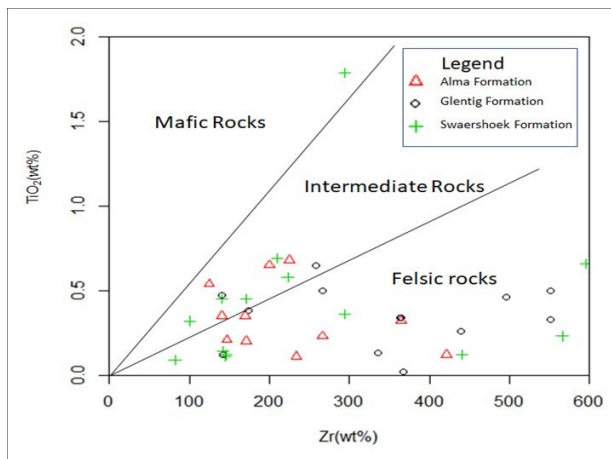


Figure 17. Binary plot of  $TiO_2$  versus Zr for samples from the Glentig, Alma and Swaershoek Formations (Background field after [54])

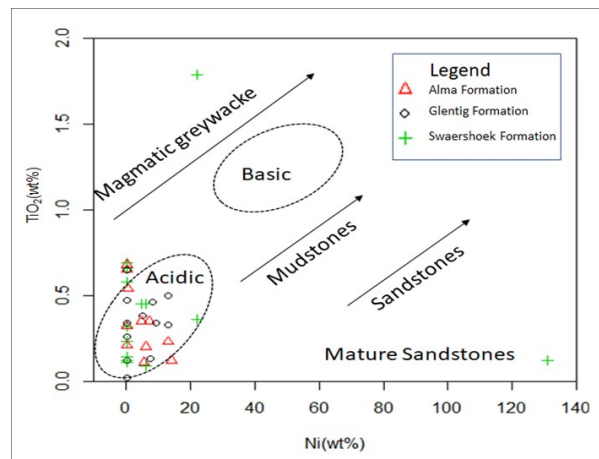


Figure 18. Binary plot of  $TiO_2$  against Ni showing the different clastic sediments and an acidic provenance (Background field after [23])

### 5.3. Tectonic setting

Several researchers have documented that the chemical compositions of siliciclastic sedimentary rocks are considerably controlled by plate tectonic settings of their provenances and depositional basins [6-8]. Thus, siliciclastic rocks originating from different tectonic settings possess terrain-specific geochemical signatures. Tectonic setting discrimination diagrams offer reliable results for siliciclastic rocks that have not been highly affected by post-depositional physical weathering, chemical weathering and metamorphic process [7,15].

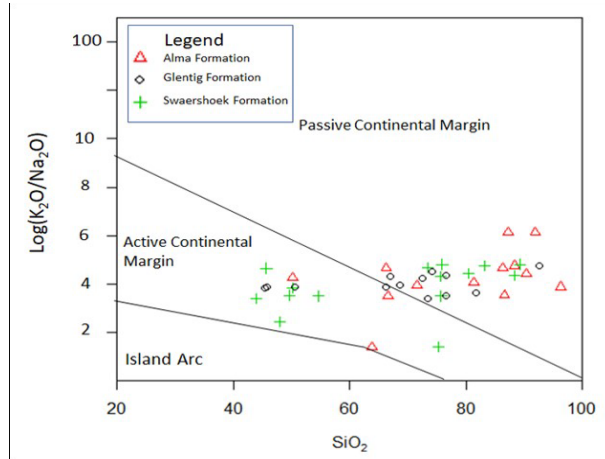


Figure 19. Binary plot of Log (K<sub>2</sub>O/Na<sub>2</sub>O) versus SiO<sub>2</sub> for the Alma, Glentig, and Swaershoek Formations (Background field after [8])

Bivariate plots of major and trace element geochemistry have been used to determine the tectonic setting of sandstones [6,8,14,25]. The binary plot of SiO<sub>2</sub> versus Log (K<sub>2</sub>O/Na<sub>2</sub>O) indicated that the sediments had been derived from a passive margin and an active continental margin (Figure 19). According to [8], passive continental margin represents a quartz-rich, mineralogically mature sediments deposited in plate interiors at intracratonic basins or stable continental margins. Active continental margins represent sediments that are quartz-intermediate, derived from tectonically active continental margins or adjacent to active plate boundaries [8].

### 5.4. Paleoweathering conditions

The degree of weathering of the source rock depends mainly on the nature of the source rock, period of weathering, climatic conditions and rates of tectonic upliftment of the source region. Calcium (Ca<sup>2+</sup>), sodium (Na<sup>+</sup>) and potassium (K<sup>+</sup>) cations are mainly removed during weathering, the relative concentration of these elements left in the samples serve as the indicators of the degree of weathering. As the intensity of weathering increases, the concentration of Ca<sup>2+</sup>, Na<sup>+</sup>, K<sup>+</sup> and Sr decreases, such depletion can be attributed to the alteration of feldspars. The decrease in these ions gives rise to an increase in Fe<sup>+</sup>, Al<sup>3+</sup> and Ti. Fiantis *et al.* [11] indicated that weathering indices help to determine or unravel how much of the original concentration has been removed compared to the remaining concentration. To determine the paleoweathering conditions, [53] proposed the chemical index of weathering (CIW), chemical index of alteration (CIA) and plagioclase index of alteration (PIA) to evaluate the degree of chemical weathering.

The provenance studies have indicated that the source rock of these sediments is acidic and according to [53], the alkali contents of siliciclastic sediments are prone to depositional alteration. The ratios of K<sub>2</sub>O/Na<sub>2</sub>O and the sum of K<sub>2</sub>O+Na<sub>2</sub>O are reliable indicators of the degree of weathering. The molecular proportions of mobile and immobile oxides have been used for the determination of source rock weathering. Source rock weathering indices used in this study are the CIW, CIA, and PIA. The calculated values for these weathering indices are shown in Table 2. According to [53], the CIA is defined by the formula for the evaluation of the degree of weathering:

$$CIA = [Al_2O_3 / (Al_2O_3 + CaO^* + Na_2O + K_2O)] * 100 \quad (1)$$

wherein CaO\* is the content of CaO incorporated in the silicate fraction.

The chemical index of alteration represents the ratio of former minerals to secondary minerals. CIA values for unweathered rocks are typically less than 50, range between 50 and 80 for weathered rocks, and can reach 100 for highly weathered rocks. In general, CIA values

increase as the degree of weathering increases, reaching 100 when all of the Ca, Na, and K have been leached from the weathering residue [53]. The CIA values for the studied samples ranges from 34.16 to 97.93, averaging 63.88 (Table 2). These CIA values revealed that the samples have undergone moderate to the high degree of weathering. This in line with the proximity of the source of the rocks which is the Bushveld Igneous Complex. The CIW of the analysed samples ranges from 81.32 to 99.83, averaging 96.61 (Table 2). These values indicate a high degree of chemical weathering. According to [52], the CIW formula is given by:

$$CIW = \left[ \frac{Al_2O_3}{Al_2O_3 + CaO + Na_2O} \right] 100 \quad (2)$$

The CIW is better as compared to other weathering indices because it involves fewer components and entails components that contain consistent geochemical demeanour during weathering. The plagioclase index of alteration (PIA) assesses the source area weathering and redistribution during diagenesis. This is attained by monitoring and quantifying progressive weathering of feldspars to clay minerals and according to [54], the formula is given as:

$$PIA = \left[ Al_2O_3 - \frac{K_2O}{Al_2O_3 + CaO + Na_2O - K_2O} \right] * 100 \quad (3)$$

The PIA values range from 54.98 to 122.22, averaging 96.16 (Table 2). This indicates moderate to intensive weathering of the feldspars. When weathering occurs, calcium is leached first then followed by potassium and then sodium (Figure 20). The plagioclase index of alteration (PIA) denotes that, if the determined value after the calculation is less than 50 then the sample is fairly fresh, thus it has not been subjected to intense weathering [53]. While a PIA value between 50 and 100 does show some degree of weathering, thus close to 50 is least altered and close to 100 shows a high degree of alteration (Table 4). The PIA values range from 54.98 to 122.22, indicating that most of the samples are altered. The bivariate diagrams show a weak correlation of the feldspars with the PIA (Figure 20). Nesbitt and Young [24] reported that the weak correlation of the feldspars with PIA could be attributed to potassium leaching.

Table 4. Indices of weathering calculated from the major elements

Samples	Lithology	Formation	CIA	PIA	CIW
PEB 001	Sandstone	Alma	77.04	97.25	98.00
PEB 002	Sandstone	Alma	73.84	98.75	99.18
PEB 003	Sandstone	Alma	73.44	97.76	98.52
PEB 004	Sandstone	Alma	75.23	99.08	99.37
PEB 005	Sandstone	Alma	74.59	98.81	99.20
PEB 006	Sandstone	Alma	78.33	97.22	97.92
PEB 007	Sandstone	Alma	73.59	95.95	97.25
PEB008	Sandstone	Alma	34.16	106.45	94.97
PEB009	Sandstone	Alma	58.06	93.41	97.94
PEB010	Sandstone	Alma	79.18	98.73	99.05
PEB011	Sandstone	Alma	66.47	84.81	90.24
PEB012	Sandstone	Alma	66.01	96.69	98.31
PEB013	Sandstone	Alma	61.43	94.44	97.73
PEB 016	Sandstone	Alma	74.49	98.71	99.13
MEL 0012	Sandstone	Glentig	51.00	54.98	84.93
MEL 0015	Sandstone	Glentig	69.31	97.90	98.80
MEL 0016	Sandstone	Glentig	74.02	89.96	92.46
MEL 0017	Sandstone	Glentig	78.47	91.82	93.38
MEL 0018	Sandstone	Glentig	39.50	101.28	99.34
MEL 026	Sandstone	Glentig	76.00	99.13	99.40
MELS 0016	Sandstone	Glentig	52.02	93.33	99.40
MEL 0025	Sandstone	Glentig	70.95	98.70	99.22
MEL 0019	Sandstone	Glentig	97.03	99.83	99.83

Samples	Lithology	Formation	CIA	PIA	CIW
MEL0020	Sandstone	Glentig	84.56	99.53	99.62
MEL0021	Sandstone	Glentig	78.61	97.89	98.42
MEL0022	Sandstone	Glentig	78.45	99.29	99.48
MEL0023	Sandstone	Glentig	86.34	93.72	94.30
MEL0024	Sandstone	Glentig	97.93	99.69	99.70
MEL0026	Sandstone	Swaershoek	65.81	75.56	81.32
MEL0027	Sandstone	Swaershoek	76.56	93.56	95.12
MEL0028	Sandstone	Swaershoek	48.18	122.22	98.85
MEL0029	Sandstone	Swaershoek	82.47	99.26	99.42
MEL0030	Sandstone	Swaershoek	92.90	98.29	98.39
MEL0031	Sandstone	Swaershoek	88.52	99.63	99.67
MEL0032	Sandstone	Swaershoek	35.52	103.98	97.08
MEL0033	Sandstone	Swaershoek	77.69	98.91	99.22
MEL0034	Sandstone	Swaershoek	43.19	108.33	97.80
MEL0035	Sandstone	Swaershoek	57.06	94.77	98.57
MEL0036	Sandstone	Swaershoek	75.80	98.47	98.94
MEL0037	Sandstone	Swaershoek	56.73	95.60	98.87
MEL0038	Sandstone	Swaershoek	64.50	95.16	97.65

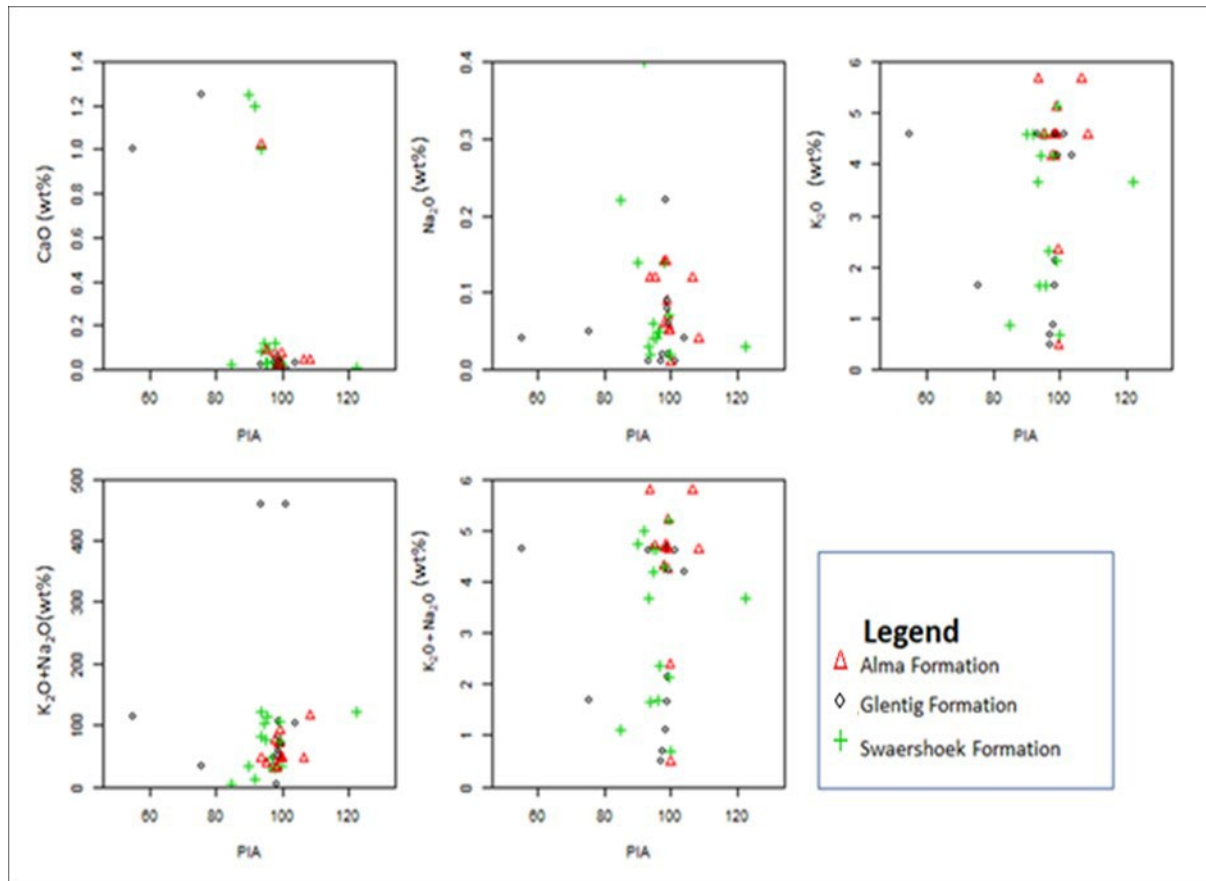


Figure 20. Bivariate diagrams showing the mobility of elements during weathering of feldspars (PIA) in the samples from Glentig, Alma and Swaershoek Formations

The  $Al_2O_3$ –( $CaO+Na_2O$ )– $K_2O$  (represented as A–CN–K) ternary diagram of [24] is another useful approach for assessing the composition of source rock and mobility of elements during chemical weathering of source material and post-depositional chemical modifications. The A–CN–K ternary plot of the sandstones (Figure 21) was plotted to unravel the compositional

changes of the sandstones that are related to chemical weathering, diagenesis and source rock composition.

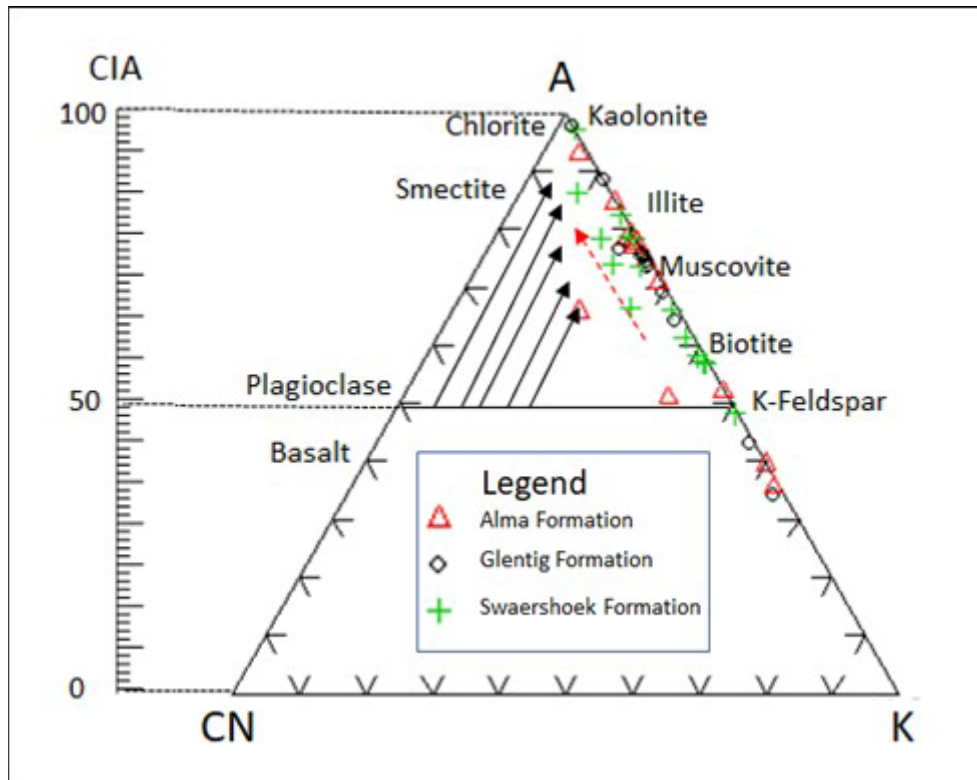


Figure 21. A-CN-K ternary diagram of molecular proportions of  $\text{Al}_2\text{O}_3$ -( $\text{CaO}+\text{Na}_2\text{O}$ )- $\text{K}_2\text{O}$  for Swaershoek, Alma and Glentig Formations (Background field after [24]). The CIA scale shown at the left side is for comparison

The  $\text{Al}_2\text{O}_3$ -( $\text{CaO}+\text{Na}_2\text{O}$ )- $\text{K}_2\text{O}$  composition of the studied samples was plotted on the A-CN-K ternary diagram background fields of [24]. The arrows indicate the weathering path for gabbro, tonalite, granodiorite, adamellite and granite, respectively. The A-CN-K diagrams of the sandstones show that all the samples plotted above the line joining plagioclase and K-feldspar (Figure 21). The weathering trendline of the sandstones is closer to the A-K boundary, signifying the silicates (i.e. feldspar) have experienced intense or high weathering resulting in the leaching of  $\text{Ca}^{2+}$  and  $\text{Na}^+$  out of plagioclase. Furthermore, the sandstones' weathering trendline (red dotted arrow in Figure 21) is parallel with the A-K boundary and slightly extends toward the A apex, indicating K leaching and Al enrichment. This suggests that additional weathering has resulted in the decomposition of K-bearing minerals (biotite, illite, and potassium feldspar). Thus, kaolinite dominates the secondary clay minerals. In the sandstones, kaolinite, illite and smectite are the main weathering products.

## 6. Conclusions

The provenance, tectonic setting, and paleoweathering conditions of the sandstones from the Swaershoek and Alma Formations (Waterberg Group) and Glentig Formation have been assessed using inorganic geochemical studies. The major oxide and trace element concentrations in the sandstones show significant variation in composition across the samples. The discrimination diagrams based on major oxide geochemistry shows that the sandstones are of a felsic/silicic source provenance with little contribution from the intermediate igneous provenance, suggesting that they were mostly derived from a cratonic interior or recycled orogen. These sediments could have been derived from the whining stages of the emplacement of the Bushveld igneous complex. The tectonic setting discrimination diagrams support the passive-

active continental margin setting of the provenance. The aforementioned characteristics indicate that the sandstones were deposited on a passive continental margin that received an enormous amount of immature detritus from the hinterland areas. The CIA and PIA values, as well as the A-CN-K ternary diagram suggest that the source area of the sandstones was subjected to moderate to intense weathering conditions.

**Acknowledgments:** *The authors thank the Mining Qualification Authority of South Africa for funding this project.*

## References

- [1] Callaghan CC, Eriksson PG, Snyman CP. The sedimentology of the Waterberg Group in the Transvaal, South Africa: an overview. *Journal of African Earth Sciences* 1991; 13: 121–139.
- [2] SACS, South African Committee for Stratigraphy, Stratigraphy of South Africa. Part 1. Lithostratigraphy of the Republic of South Africa, South West Africa/Namibia and the Republics of Bophuthatswana, Transkei and Venda. Handbook of the Geological Survey of South Africa, 1980: 1–8.
- [3] Salvador A. Unconformity-bounded stratigraphic units. *Geological Society of America Bulletin*, 1949; 98: 1544–1552.
- [4] Johnson MR, van Vuuren, C, Visser J, Cole D, de Wickens H, Christie A, Roberts D. The Foreland Karoo Basin, South Africa., In: R. Selley (Editor). *African Sedimentary Basins of the World*, Elsevier, Amsterdam, 1997; 3: 269–317.
- [5] Boggs SJ. *Principles of Sedimentology and Stratigraphy*, 3rd Edition. Prentice Hall, New Jersey, 2009: 153–1726.
- [6] Bhatia MR. Plate tectonics and geochemical composition of sandstones. *Journal of Geology*, 1983; 91: 611–627.
- [7] McLennan SM, Taylor SR, Eriksson KA. Geochemistry of Archaean shales from the Pilbara Supergroup, Western Australia. *Geochim. Cosmochim. Acta*, 1983; 47(7): 1211–1222.
- [8] Roser BP, Korsch RJ. Provenance signatures of sandstone-mudstone suites determined using discriminant function analysis of major-element data. *Chemical Geology* 1988; 67: 119–139.
- [9] Roser BP, Korsch RJ. Determination of tectonic setting of sandstone-mudstone suites using SiO<sub>2</sub> content and K<sub>2</sub>O/Na<sub>2</sub>O ratio. *Journal of Geology* 1986, 94, 635–650.
- [10] Bhatia MR, Crook KAW. Trace element characteristics of graywackes and tectonic setting discrimination of sedimentary basins. *Mineralogy and Petrology*, 1986; 92: 181–193.
- [11] Fiantis D, Nelson M, Shamshuddin J, Goh TB, Van Ranst E. Determination of the Geochemical Weathering Indices and Trace Elements Content of New Volcanic Ash Deposits from Mt. Talang (West Sumatra) Indonesia. *Eurasian Soil Science*, 2010; 43: 1477–1485.
- [12] Hayashi KI, Fujisawa H, Holland HD, Ohmoto, H. Geochemistry of ~1.9 Ga sedimentary rocks from northeastern Labrador, Canada. *Geochimica et Cosmochimica Acta*. Pergamon, 1997; 61: 4115–4137.
- [13] Dickinson WR, Beard LS, Brakenridge GR, Erjavec JL, Furgeson RC, Inman KF, Knepp RA, Lindberg FA, Ryberg PT. Provenance of North American Phanerozoic sandstones in relation to tectonic setting. *Geological Society of America Bulletin*, 1983; 94: 222–235.
- [14] McCann T. Petrological and geochemical determination of provenance in the southern Welsh Basin. In: AC Morton, SP Todd, PDW Haughton (Eds.). *Developments in Sedimentary Provenance*. Geological Society Special Publication, 1991; 57: 215–230.
- [15] McLennan SM, Hemming S, McDaniel DK, Hanson GN. Geochemical approaches to sedimentation, provenance and tectonics. In: M.J. Johnson and A. Basu, (Eds.). *Processes controlling the composition of clastic sediments*. Geological Society of American Special Paper, 1993; 32: 21–40.
- [16] Cullers RL, Podkovyrov VL. Geochemistry of the Mesoproterozoic Lakhanda shales in southeastern Yakutia, Russia: implications for mineralogical and provenance control and recycling. *Precambrian Research*, 2000; 104: 77–93.
- [17] Condie KC, Lee D, Farmer GL. Tectonic setting and provenance of the Neoproterozoic Uinta Mountain and Big Cottonwood groups, northern Utah: Constraints from geochemistry, Nd isotopes and detrital modes. *Sedimentary Geology*, 2001; 141: 443–464.
- [18] Hessler AM, Lowe DR. Weathering and sediment generation in the Archean: An integrated study of the evolution of siliciclastic sedimentary rocks of the 3.2 Ga Moodies Group, Barberton Greenstone Belt, South Africa. *Precambrian Research*, 2006; 151: 185–210.

- [19] Aragón EP, Lucio DE, Castro F, Rabbia A, Coniglio O, Demartis J, Hernando M, Cavarozzi I, Aguilera CE, Yolanda E. The Farallon-Aluk ridge collision with South America: Implications for the geochemical changes of slab window magmas from fore- to back-arc. *Geoscience Frontiers*, 2013; 4: 377–388.
- [20] Baiyegunhi C, Liu K, Gwavava O. Geochemistry of sandstones and shales from the Ecca Group, Karoo Supergroup, in the Eastern Cape Province of South Africa: Implications for provenance, weathering and tectonic setting. *Open Geosciences*, 2017; 9: 340–360.
- [21] Baiyegunhi TL, Liu K, Gwavava O, Baiyegunhi C, Rapholo DD. Geochemistry of the mudrocks and sandstones from the Bredasdorp Basin, offshore South Africa: Implications for tectonic provenance and paleoweathering. *Open Geosciences*, 2021; 13: 1187–1225.
- [22] Denge E, Baiyegunhi C. Geochemical and Petrographical Characteristics of the Madzaringwe Formation Coal, Mudrocks and Sandstones in the Vele Colliery, Limpopo Province, South Africa: Implications for Tectonic Setting, Provenance and Paleoweathering. *Applied Sciences*, 2021; 11: 2782–2803.
- [23] Floyd PA, Winchester JA, Park RG. Geochemistry and tectonic setting of Lewisian clastic metasediments from the Early Proterozoic Loch Maree Group of Gairloch, NW Scotland. *Precambrian Research*, 1989; 45: 203–214.
- [24] Nesbitt HW, Young GM. Prediction of some weathering trends of plutonic and volcanic rocks based upon thermodynamic and kinetic consideration. *Geochimica et Cosmochimica Acta*, 1984; 48: 1523–1534.
- [25] Toulkeridis T, Clauer N, Kröner A, Reimer T, Todt W. Characterization, provenance, and tectonic setting of Fig Tree greywackes from the Archaen Barberton Greenstone Belt, South Africa. *Sedimentary Geology*, 1999; 124: 113–129.
- [26] Bracciali L, Marroni M, Pandolfi L, Rocchi S. Geochemistry and Petrography of Western Tethys Cretaceous sedimentary covers (Corsica and Northern Apennines): from source areas to configuration of margins. *Geological Society of America Special Paper*, 2007; 420: 73–93.
- [27] Jansen H. Volcanic rocks and associated sediments in the southern portion of the Waterberg basin. *Annals of Geological Survey of South Africa*, 1970; 8: 53–61.
- [28] Jansen H. The Waterberg and Soutpansberg groups in the Blouberg area, northern Transvaal. *Transactions of the Geological Society of South Africa*, 1976; 79: 281–291.
- [29] Cheney ES, Twist D. The Waterberg “Basin” – A reappraisal. *Transactions of the Geological Society of South Africa*, 1986; 89: 353–360.
- [30] Masango SM. Physical volcanology of the Rooiberg Group near Loskop Dam, Mpumalanga, South Africa. MSc dissertation, University of Pretoria, 2014; 1–156.
- [31] Catuneanu O, Wopfner H, Eriksson PG, Cairncross B, Rubidge BS, Smith RMH, Hancox PJ. The Karoo basins of south-central Africa. *Journal of African Earth Sciences*, 2005; 43: 211–253.
- [32] Dorland HC, Beukes NJ, Gutzmer J, Armstrong RA. Precise SHRIMP U-Pb zircon age constraints on the lower Waterberg and Soutpansberg Groups, South Africa. *South African Journal of Geology*, 2006; 109: 139–156.
- [33] Johnson MR, van Vuuren, CJ, Visser JNJ, Cole DI, Wickens H, Christie ADM, Roberts DL, Brandl G. Sedimentary rocks of the Karoo Supergroup. In: M. R. Johnson, C. R. Anhaeusser and R. J. Thomas (Eds.). *The Geology of South Africa*, Geological Society of South Africa and Council for Geoscience, 2006; 461–499.
- [34] Callaghan CC. The Waterberg Basin: its evolution, sedimentation and mineralisation. *Geological Society of South Africa*, 1986; 759–762.
- [35] De Kock MO. Palaeomagnetism of the lower two unconformity-bounded sequences of the Waterberg Group, South Africa: Towards a better-defined apparent polar wander path. *South African Journal of Geology*, 2006; 109: 157–182.
- [36] Barker OB, Brandl G, Callaghan CC, Eriksson PG, van der Nuet M. The Soutpansberg and Waterberg Groups and the Blouberg Formation, South Africa. *South African Journal of Geology*, 2006; 109: 301–317.
- [37] Lenhardt N, Eriksson PG. Volcanism of the Palaeoproterozoic Bushveld Large Igneous Province: The Rooiberg Group, Kaapvaal Craton, South Africa. *Precambrian Research*, 2012; 214: 82–94.
- [38] Martini JEJ. The Loskop Formation and its relationship to the Bushveld Complex, South Africa. *Journal of African Earth Sciences*, 1998; 27: 193–222.
- [39] Mtimkulu MN. A provisional basinal study of the Waterberg-Karoo, South Africa. MSc dissertation, University of Pretoria, 2009; 1–146.
- [40] Salvador A. Unconformity-bounded stratigraphic units. *Geological Society of America Bulletin*, 1987; 98: 232–237.

- [41] Chang KH. Unconformity-bounded stratigraphic units. *Geological Society of America Bulletin*, 1975; 86: 1544–1552.
- [42] Whittaker A, Cope JCW, Cowie JW, Gibbons W, Hailwood EA, House MR, Jenkins DG, Rawson PF, Rushton AWA, Smith DG, Thomas AT, Wimbledon WA. Guide to the stratigraphical procedure. *Journal of Geological Society of London*, 1991; 148: 813–824.
- [43] Maré LP, Eriksson PG, Améglio L. A palaeomagnetic study of the lower part of the Palaeoproterozoic Waterberg Group, South Africa. *Journal of African Earth Sciences*, 2006; 44: 21–36.
- [44] Du Plessis C. New perspectives on early Waterberg Group sedimentation from Gatkop area, north-western Transvaal South Africa. *South African Journal of Geology*, 1987; 90: 395–408.
- [45] Floyd PA, Leveridge BE. A tectonic environment of the Devonian Gramscatho basin, south Cornwall: framework mode and geochemical evidence from turbiditic sandstones. *Journal of the Geological Society*, 1987; 144: 531–542.
- [46] Rudnick RL, Gao S. Composition of the continental crust. *Treatise of Geochemistry*, 2003, 3: 49–64.
- [47] Dickinson WR. Interpreting provenance relations from detrital modes of sandstones. In: G Zuffa (Ed.). *Provenance of Arenites*. Reidel, Dordrecht, 1985; 333–361.
- [48] Folk RL. *Petrology of sedimentary rocks*: Hemphill Publishing Company, Austin TX, 1974; 1–182.
- [49] Basu AS, Suttner LJ, James WC, Mack GH. Re-evaluation of the use of undulatory extinction and crystallinity in detrital quartz for provenance interpretation. *Journal of Sedimentary Petrology*, 1975; 45: 873–882.
- [50] Dabbagh ME, Rogers JJ. Depositional environments and tectonic significance of the Wajid sandstone of southern Saudi Arabia. *Journal of African Earth Sciences*, 1983; 24: 47–57.
- [51] Pettijohn FJ, Potter PE, Siever R. *Sand and Sandstone*. Springer, New York, 1987; 553pp.
- [52] Weltje GJ, von Eynatten H. Quantitative provenance analysis of sediments: Review and outlook. *Sedimentary Geology*, 2004; 171: 1–11.
- [53] Nesbitt HW, Young GM. Early Proterozoic climates and plate motions inferred from major element chemistry of lutites. *Nature*, 1982; 299: 715–717.
- [54] Hayashi K, Fujisawa H, Holland HA, Ohmoto H. Geochemistry of ~1.9 Ga sedimentary rocks from north-eastern Labrador, Canada. *Geochimica et Cosmochimica Acta*, 1977; 61: 4115–4137.

---

*To whom correspondence should be addressed: professor Christopher Baiyegunhi, Department of Geology and Mining, University of Limpopo, Private Bag X1106, Sovenga 0727, Limpopo Province, South Africa, E-mail: [christopher.baiyegunhi@ul.ac.za](mailto:christopher.baiyegunhi@ul.ac.za)*